ELSEVIER

Chemical Geology 189 (2002) 135–163

CHEMICAL GEOLOGY
INCLUDING
ISOTOPE GEOSCIENCE

www.elsevier.com/locate/chemgeo

A mineralogical and geochemical study of element mobility in sulfide mine tailings of Fe oxide Cu–Au deposits from the Punta del Cobre belt, northern Chile

Bernhard Dold [a,b,*], Lluis Fontboté [b]

[a] *CAM, Earth Sciences Department, University of Lausanne, 1015 Lausanne, Switzerland*
[b] *Earth Sciences Department, University of Geneva, Rue des Maraîchers 13, 1211 Geneva 4, Switzerland*

Received 25 January 2001; accepted 27 February 2002

Abstract

Two flotation tailings sites (Ojancos and P. Cerda) from the Fe oxide Cu–Au Punta del Cobre belt, south of Copiapó, Atacama desert, northern Chile, are geochemically (largely using sequential extractions) and mineralogically compared. Main ore minerals are pyrite, magnetite and/or hematite and chalcopyrite. Gangue is dominantly calcite with minor quartz. The host silicate assemblage is largely controlled by hydrothermal alteration and consists of variable amounts of the following minerals: K-feldspar ± Ca-amphibole ± biotite ± sericite ± chlorite ± tourmaline ± epidote ± quartz. In this study, both the Ojancos and the P. Cerda tailings were deposited in valley dam impoundments and when they were filled, new tailings were deposited upstream. As a result, high quantities of seepage migrated downstream into the older tailings impoundment. At Ojancos, the recent upstream tailings have excess of acid potential (7.1 wt.% calcite and 3.5 wt.% pyrite), whereas the older downstream tailings are characterized by alternations of several meter-thick intervals with high neutralizing potential (about 40 wt.% calcite and 2 wt.% pyrite) and intervals with high acid potential (about 3 wt.% calcite and 4 wt.% pyrite). Acid mine drainage (AMD) with the precipitation of schwertmannite (pH 3.15) and chalcoalumite (pH 4.9) flows out at the interface between the uphill and downstream tailings. Strong downstream element transport is taking place and contributes to the formation of the cementation zone (mainly gypsum, ferrihydrite and goethite, and locally jarosite) in the older downstream impoundment. The cementation zone (pH = 4) shows strong enrichment of heavy metals (e.g., up to 6800 ppm Cu, 680 ppm Zn, 1100 ppm As), mainly adsorbed and as secondary sulfides (e.g., covellite). In contrast, at the P. Cerda, tailings impoundment carbonates are homogeneously distributed and the overall neutralization potential exceeds the acid potential (average of about 10 wt.% calcite and up to 2.5 wt.% pyrite). The up to 5-m thick oxidation zones (paste pH = 6.9–8.3) at P. Cerda are characterized by interlayering of coarser dark gray unoxidized layers with fine-grained, Fe(III) hydroxide-rich, ochre to red-brown colored horizons. The hyperarid climate dries out first the coarse, sulfide-rich horizons of the tailings and limits so the oxidation, which is restricted to the fine-grained, due to their higher moisture retention capacity. However, results indicate that during operation an important element transfer from the younger upstream tailings to the older downstream tailings impoundment took place, possibly by sorptive transport at ferric polymers or colloids in the form of neutral mine drainage (NMD). This would explain the metal enrichments in the cementation zone, which are mainly associated to the exchangeable fraction and not as secondary sulfides. This results, in both cases (in Ojancos mainly as AMD and in P. Cerda mainly as NMD), in Fe(III) input as ferric cation, as ferric polymer, or

* Corresponding author. Sciences de la Terre, CAM BFSH-Centre d'Analyse Minerale, Earth Sciences Department, Universite de Lausanne, CH-1015 Lausanne, Switzerland. Fax: +21-692-4315.
E-mail address: Bernhard.Dold@cam.unil.ch (B. Dold).

PII: S0009-2541(02)00044-X

CO_3 complexes to the downstream impoundment. This constitutes a very effective acid potential transfer to the older downstream material because oxidation via input of external Fe(III) produces 16 mol of protons per mol FeS_2, i.e., eight times more than via oxidation with oxygen. In addition, the created acidity favors dissolution of the abundant Fe oxides magnetite and hematite of this ore deposit type providing so additional Fe(III) for sulfide oxidation.

Keywords: Fe oxide Cu–Au deposits; Tailings; Carbonates; Acid mine drainage (AMD); Enrichment; Cementation zone; Schwertmannite; Ferrihydrite; Sequential extractions

1. Introduction

The formation of acid mine drainage (AMD) subsequent to sulfide oxidation is the main environmental problem facing the mining industry today. To prevent a net acid production, the silicate and principally the carbonate mineral assemblage are the key parameters to neutralize the liberated protons during sulfide oxidation and subsequent hydrolysis of secondary phases. To calculate the quantity of carbonates necessary for the neutralization of the potentially formed acid, a broad range of standard static test methods were developed and are reviewed in White et al. (1999). The carbonate distribution may also have an important influence to develop the maximum neutralization potential. The importance of carbonates in the sulfide oxidation has controversial aspects. Lapakko et al. (1997) demonstrated in laboratory studies with mixing of acid-producing tailings with limestone and Holmström et al. (1999) with carbonate-rich tailings that high carbonate content may decrease the sulfide oxidation rates. This is generally thought to be related to the coating of sulfide by secondary ferric phases. In contrast, Evangelou and Huang (1994) suggest that CO_3 may even promote pyrite oxidation by promoting electron transfer via pyrite surface Fe(II)–CO_3 complexes.

In addition to primary mineralogy, another important parameter for the formation of secondary minerals, and for the formation of acidity due to hydrolysis, is climate. In humid climates, the subsequent to sulfide oxidation and neutralization reactions liberated elements are transported downwards to more reducing conditions (below the groundwater level). This often results in retention of these elements by pH-controlled sorption processes and/or precipitation of secondary minerals (e.g., Fe oxides and Cu sulfides). In contrast, in arid climates, an upward migration to more oxidizing conditions via capillary force may develop (Dold and Fontboté, 2001). These authors show that in strongly acidic oxidation zones (paste pH in the oxidation zone 1.7–4), the upward element transport leads to the formation of water-soluble sulfate minerals at the surface of porphyry copper tailings. In the case of carbonate-rich tailings, where the acidity produced by sulfide oxidation is neutralized and pH values are near neutral (e.g., Blowes et al., 1998), sorption processes limit strongly the mobility of the bivalent metal cations.

Another parameter, which may play a role in the element mobility in the tailings impoundments, is the water input. In areas with pronounced topography (e.g., Chile), valley dam construction techniques are mainly used and consist of tailings deposition upstream from a dam closing the valley. Continuous operation of the flotation plant beyond the originally planned impoundment capacity makes additional space necessary to deposit the tailings. An often-applied solution is to construct a new valley dam impoundment directly upstream of the older one. As a result, seepage can migrate from the upstream new tailings into the older downstream tailings impoundment during operation. This impoundment construction type can be encountered in the whole Pacific Rim and in most orogenic regions of the world making necessary a good understanding of the influence of the seepage in the geochemical processes taking place in the impoundments.

In this work, two case studies of tailings impoundments (Ojancos and P. Cerda) of calcite-rich Fe oxide Cu–Au deposits from the Punta del Cobre belt, Copiapó, northern Chile, are compared (Figs. 1 and 2). Pyrite and chalcopyrite are the main sulfide minerals in the mines of the Punta del Cobre belt and calcite is locally important as gangue mineral (Marschik, 1996;

Marschik and Fontboté, 2001b). The studied sites are characterized by inhomogeneous (Ojancos) and homogeneous (P. Cerda) calcite distribution and in both sites new valley dam impoundments were constructed uphill of older ones so that seepage developed. The configuration of the selected tailings allows to study in detail (1) the geochemical and mineralogical behavior of tailings from calcite-rich Fe oxide Cu–Au deposits deposited under arid climates, (2) the influence on mineralogical evolution and element mobility of different water input regimes (including seepage of recent acid mining drainage and neutral mine waters) and (3) the influence of carbonate distribution. In addition, at Ojancos one of the tailings impoundments was in operation during sampling whereas at P. Cerda operation had ceased 20 years before, providing additional comparison possibilities.

2. Regional geology and ore geology

The Cretaceous Fe oxide Cu–Au Punta del Cobre belt in northern Chile includes the mining districts of Punta del Cobre, Ladrillos, Las Pintadas, as well as the newly discovered giant deposit at the La Candelaria mine (Fig. 1). The area has been a traditional center of the Chilean middle-size mining industry since the early 1900s. Copper ores have been processed by flotation since 1929. Recent studies have focused on the genesis of mineralization and alteration in the Punta del Cobre Belt (Marschik, 1996; Marschik and Fontboté, 2001b; Ryan et al., 1995). The Punta del Cobre Formation, exposed in the core of the Tierra Amarilla anticline, consists mainly of altered volcanic and volcanoclastic rocks. It includes epiclastic breccias, sandstone, siltstone and, in its upper part, chert and limestone. Marschik and Fontboté (1996) differentiated five main alteration types at the Punta del Cobre belt. An early episode of hydrothermal alteration caused extensive albitization (albite–quartz–chlorite, ± sericite ± calcite) which was locally superimposed by potassic alteration (K-feldspar–quartz–chlorite/biotite ± sericite ± calcite ± tourmaline). The other three alteration types are located adjacent to the middle Cretaceous batholith in the western part of the area. They are characterized from west to east by the mineral assemb-

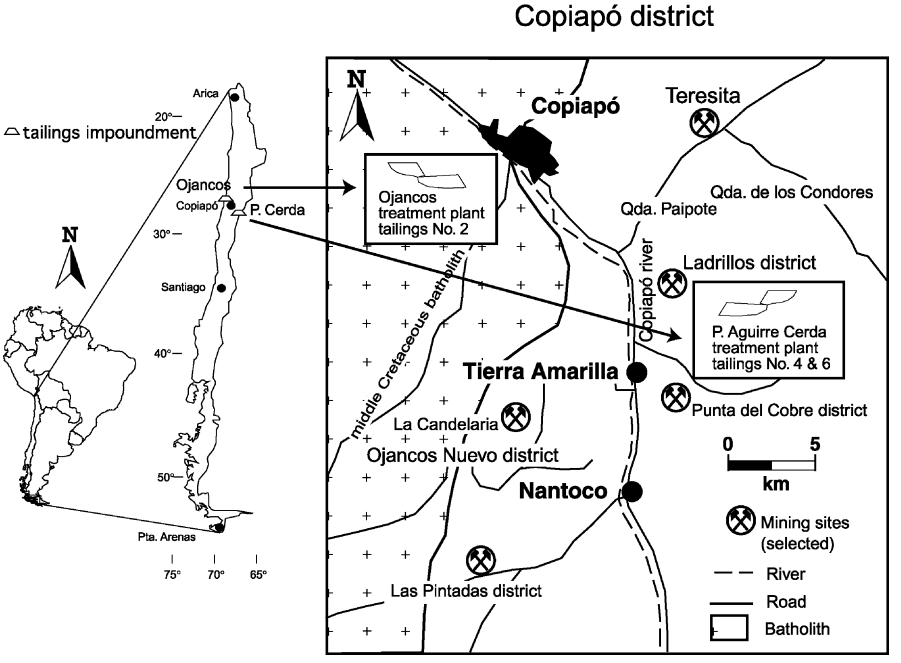

Fig. 1. Overview of the sampled tailings impoundments from the Ojancos flotation plant and the P. Cerda flotation plant, Copiapó District, Northern Chile.

lages of Ca-amphibole ± biotite ± sericite, biotite ± chlorite ± sericite ± epidote and epidote chlorite ± quartz ± calcite.

The mineralization at Punta del Cobre is characterized by a simple hypogene mineral assemblage including (in decreasing order of importance) pyrite, magnetite or hematite and chalcopyrite. Sphalerite is observed very locally. Gangue is dominantly calcite with minor quartz (Marschik, 1996). A general trend of increased calcite content with greater distance from the middle Cretaceous Andean batholith is observed in the different deposits in the region. Thus, the Teresita ores (mantos emplaced in limestone) and the mines in the eastern part of the Punta del Cobre belt (e.g., Socavón Rampla, Augustina, and Bateas) have higher calcite contents than the La Candelaria mine and the Las Pintadas district (Fig. 1). Additionally, the first mined upper parts of the sequence of the Punta del Cobre belt were, in general, richer in calcite than the lower, quartz-rich areas (Marschik and Fontboté, 2001a).

3. Climate

The Copiapó valley is located in the Atacama desert (27.3°S, 70.4°W). The climate is hyperarid with an average rainfall from 1904 to 1988 of 20.7 mm/year. The averages of maximal, median and minimal absolute temperature values in the period of

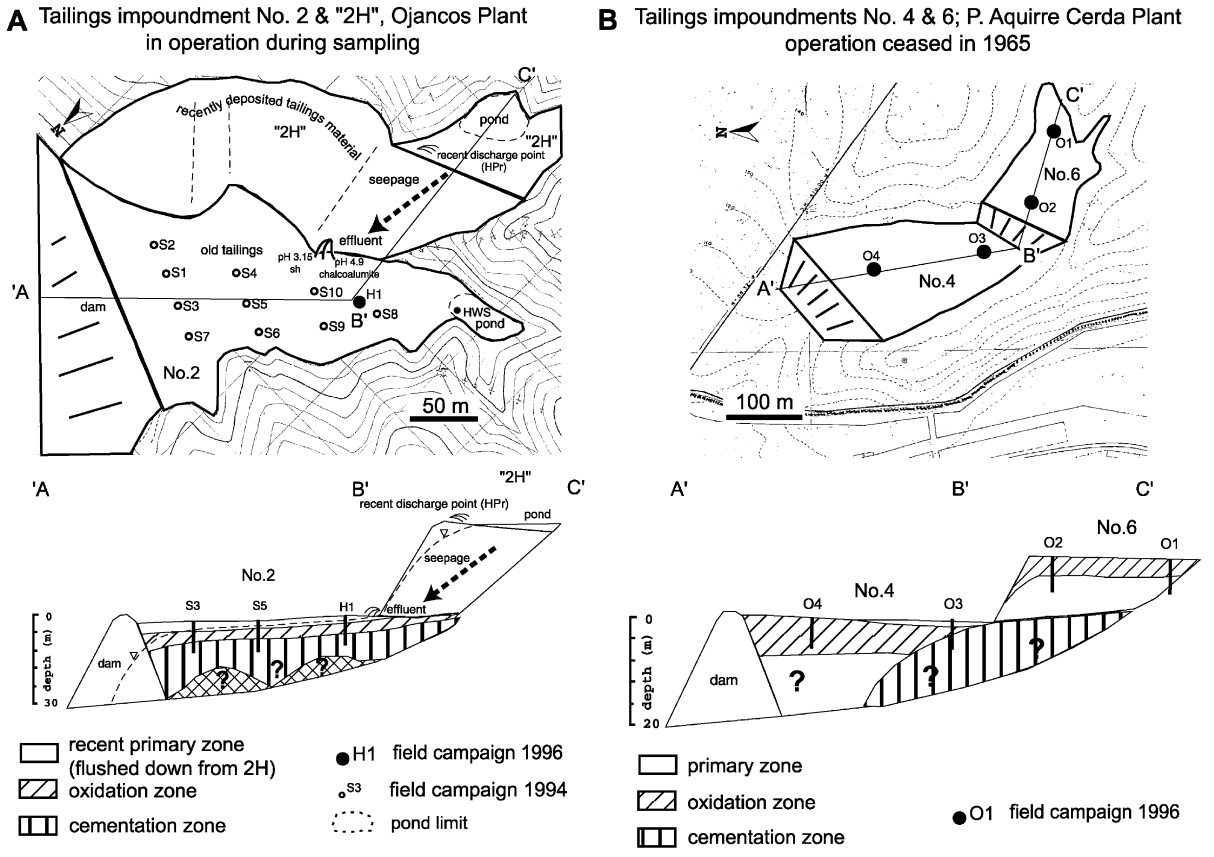

Fig. 2. (A) Overview of the tailings impoundment no. 2 of the Ojancos flotation plant with the recent deposition of the tailings at "2H" at the hillside of impoundment no. 2. The deposition at "2H" was active during sampling. (B) Overview of the tailings impoundment nos. 4 and 6x of the flotation plant P. Cerda. These tailings are out of operation since 1965.

1946–1977 are 32.1, 15.6 and −0.4 °C, respectively. The average of the relative humidity in the period from 1946 to 1977 measured at 8 a.m. was 87.5%, at 2 p.m. 51.0% and at 8 p.m. 65.7%, reflecting the frequent presence of morning fog, which disappears generally at noon. Exceptional, strong rainfall may occur in association with the El Niño phenomenon, as in 1997. No data are available for evaporation rates. It must be assumed that the evaporation strongly exceeds the rainfall.

4. Description of the studied mine tailings impoundments

4.1. Tailings impoundment no. 2 from the Ojancos plant, Sali Hochschild, Copiapó, northern Chile

4.1.1. Treatment processes

The Ojancos mineral treatment plant is located within the city of Copiapó directly behind the campus of the University of Atacama. This installation was owned and managed by the Compañia Minera Sali Hochschild. It was the first treatment plant in the Copiapó mining district (1911) and treated during its long history copper, gold and silver ores mainly by alkaline flotation (pH 11), minor cyanidation and heap leaching. The flotation plant started operation in 1936. Before 1982, all treated material was bought from external mines (Zamora, 1993). Although there are no reliable records regarding which mines the ore came from, it is reasonable to assume that prior to 1982, the plant processed ore primarily from the Punta del Cobre belt, i.e., possibly mainly from the Teresita, Pintadas, Augustina, Socavón Rampla, Manto Verde and Bateas mines. Since 1982, the Ojancos plant has only treated ore from the Teresita and Las Pintadas mines (Fig. 1); plant operations shut down in 1998.

4.1.2. Tailings impoundment history and geotechnical situation

The Ojancos mineral treatment plant has four tailings impoundments. The present work studies tailings impoundment no. 2 which was in operation during the period of 1967–1977 (Figs. 2 and 3A). The historical reports indicate that the flotation tailings deposited between 1967 and 1977 in the "old" downstream Ojancos impoundment no. 2 most likely come from the Punta del Cobre belt. After 1977, there was a period of no deposition. It is situated over alluvial and fluvial alternating silty and clayey sands with gravels and conglomerate intercalations at an altitude of 100 m a.s.l. with direct hydrological connection to the Copiapó river valley. The upstream "2H" tailings deposited after 1987 and still being deposited during sampling at the hillside of impoundment no. 2 have their origin from the Teresita mine and the Pintadas district (Figs. 1–3A). For better stability, only the coarse tailings fraction (separated by cyclones) was deposited hillside, resulting in a high hydraulic conductivity. The fine fraction was deposited in tailings impoundments nos. 3 and 4, which are situated about 3 km northwest of the plant (Zamora, 1993, Hochschild, Copiapó, personal communication). The material has its origin from of ores from the Teresita and Las Pintadas mines. The recent Ojancos tailings at the hillside are referred to as "2H" to differentiate them from the original "no. 2" impoundment. Deposition of the "2H" tailings was still active during the sampling period (1994–1997). Each month, slurry with 4000 m^3 of water was deposited on the hillside above impoundment no. 2. Due to the active operation, it was not possible to sample the "2H" tailings, but the discharge point (HPr, Fig. 2) could be sampled. The dam for impoundment no. 2 is constructed mainly with coarse material from heap leaching tests on material form the Punta del Cobre district. During the original operating time of the impoundment no. 2 (1967–1982), cyanidation was not in operation (Zamora, 1993) so that the tailings in this impoundment were treated only by flotation.

4.2. Tailings impoundments nos. 4 and 6, Pedro A. Cerda treatment plant Ojos del Salado deposits, south of Copiapó

4.2.1. Treatment process

The flotation treatment plant P. Cerda (Figs. 2 and 3D) is located next to the village of Tierra Amarilla, about 15 km south of the town of Copiapó (Fig. 1). It started operation in 1929 and in 1984, it was bought by the Compañia Minera Ojos del Salado. The plant uses an alkaline flotation circuit.

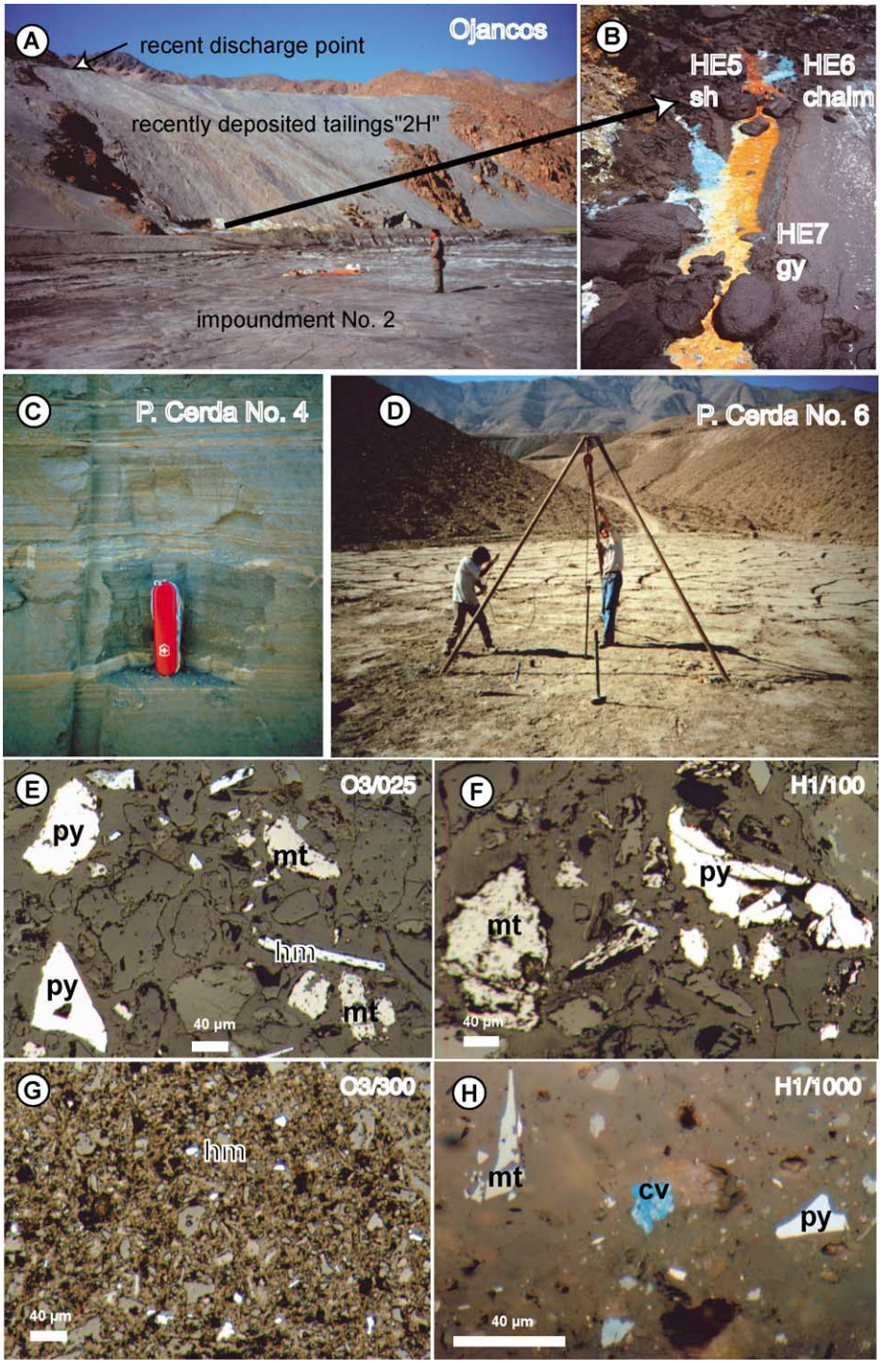
A
Ojancos
recent discharge point
recently deposited tailings"2H"
impoundment No. 2
B
HE5
sh
HE6
chalm
HE7
gy
C
P. Cerda No. 4
D
P. Cerda No. 6
E
O3/025
py
mt
hm
py
mt
40 µm
F
H1/100
py
mt
40 µm
G
O3/300
hm
40 µm
H
H1/1000
mt
cv
py
40 µm

4.2.2. Tailings impoundments history and geotechnical situation

The P. Cerda plant has presently one tailings impoundment in operation situated 1.8 km northwest of the plant, and six older tailings impoundments. The old impoundments nos. 4 and 6 were best suited for sampling (Fig. 2). The treated material has its origin in the eastern part of Punta del Cobre belt, possibly mainly from the mines Agustina, Bateas, Manto Verde and Socavón Rampla, which were the principal mines in operation during the filling of the impoundments nos. 4 and 6. The tailings impoundment no. 4 is located in a small valley closed by a dam at an altitude of 100 m a.s.l. The tailings impoundment no. 6 is situated directly upstream of the impoundment no. 4 (Figs. 2 and 3D). Tailings impoundment no. 4 stopped operation around 1965 and no. 6 was active possibly until 1975. Therefore, for an approximately 10-year period, the seepage from tailings impoundment no. 6 flowed into the tailings no. 4, i.e., in a similar configuration as at the studied tailings at Ojancos. Both tailings are located over Atacama gravels of Miocene age, with direct hydrologic connection to the Copiapó river valley.

5. Methodology

5.1. Sampling and field methods

A total of 15 cores were taken and 170 samples were obtained from the two studied sites. In the first field campaign in 1994 in the Ojancos tailings impoundment no. 2, 10 cores up to depths of 8 m were taken with percussion sampling equipment, and 101 samples were obtained. In a second field campaign in 1996, an additional core H1 of 10-m depth was sampled from the Ojancos impoundment no. 2 and four cores were sampled on the Ojos del Salado tailings impoundment nos. 4 and 6. In a third visit to Ojancos in 1997, eight samples of effluent precipitates at the foot of the recent coarse "2H" tailings were collected, pH was measured and the samples were air-dried (Fig. 3B). The tailings samples were sealed in plastic bags and stored in an ice-packed cool box. Previously, the description of mineralogical characteristics, color and grain size estimation and pH measurement (paste pH according to MEND, 1991; WTW® pH meter) were noted. The samples were transported immediately to the IDICTEC laboratories, University of Atacama, for air drying (<35 °C) and water content determination. The moisture content of all tailings samples was measured by the difference of sample weight before and after drying. The particle size distribution of selected samples were measured by a Coulter® and a Fritsch Analysette® laser particle size analyzer. The hydraulic conductivity (K) was calculated after Hazen (1893, in Hölting, 1989).

5.2. Mineralogical methods

For the description of the tailings mineralogy, the classification proposed by Jambor (1994) was used. Polished sections and polished thin sections were prepared from selected bulk samples. Samples were analyzed as bulk sample by X-ray diffraction (XRD), using a Philips 3020 diffractometer with CuKα ($\lambda = 1.54056$ Å) and a monochromator. Scan settings were 3–70° 2θ, 0.02° step size, 2-s count time per step. Procedures for identification of clay minerals followed Moore and Reynolds (1997). The poorly crystalline Fe(III) oxyhydroxides such as ferrihydrite

Fig. 3. (A) Photograph of the situation at the Ojancos impoundment no. 2 with the recently deposited tailings "2H" at the hill site. (B) AMD precipitates at the interface of both impoundments. HE5 with schwertmannite (sh) has pH 3.15, HE6 with chalcoalumite (chalm) has pH 4.9 and HE7 with gypsum (gy) has pH 4.54. Width of photo 100 cm. (C) Detail of the P. Cerda tailings no. 4. The coarser layers are essentially not oxidized, whereas the fine-grained horizons show precipitation of secondary Fe(III)hydroxides. (D) Sampling on the tailings impoundment no. 6 of the P. Cerda flotation plant. Note that despite the aridity no efflorescent salts are formed at the surface due to neutral pH (in contrast to El Salvador tailings, Dold and Fontboté, 2001). (E) Polished section with typical appearance of pyrite (py), magnetite (mt) and hematite (hm, specularite) in the primary zone of P. Cerda tailings impoundment no. 4 (sample O3/025). (F) Pyrite (py) and magnetite (mt) as dominant ore minerals in the primary zone of the Ojancos tailings impoundment no. 2 (sample H1/100). (G) Typical appearance of the fine-grained cementation zone with hematite (hm) and Fe(III) hydroxides in the P. Cerda tailings impoundment no. 4 (sample O3/300). The rounded edges of the hm grains suggest that they are affected by dissolution. (H) The fine-grained cementation zone with rounded relicts of pyrite (py) and magnetite (mt), and with secondary covellite (cv), and Fe(III) hydroxides in the Ojancos tailings impoundment no. 2 (sample H1/1000).

were detected by differential X-ray diffraction (DXRD), following the methods described by Schulze (1981, 1994). The diffractometer settings were those used by Bigham et al. (1990, 1994, 1996) and Schwertmann et al. (1995), i.e., step scanning with 0.05° 2θ step size and 20-s counting time per step. The samples from the cementation zone selected for DXRD were attacked by 0.2 M ammonium oxalate, pH 3, 80 °C, 2 h. Scans were measured before and after treatment. The treated scan was intensity corrected and then subtracted from the untreated scan. The resulting DXRD pattern was used for mineral determination. The acid mine drainage precipitates were characterized by XRD with the same settings as mentioned above. The mineral morphology and qualitative element composition of the acid mine drainage precipitates were studied by scanning electron microscopy (SEM-EDS).

5.3. Geochemical methods

5.3.1. Mixed acid digestion (HNO_3, HF, $HClO_4$, HCl)

In a preliminary phase of the investigation, tailings samples from seven representative drill cores (S1, S2, S3, S6, S7, S8 and S9; for location, see Fig. 2) were completely digested with a mixture of HNO_3, HF, $HClO_4$ and HCl. Metal concentrations in the solutions were measured by ICP-MS and ICP-AES (Dold et al., 1996). The objective was to obtain an overall insight in the tailings composition.

5.3.2. Sequential extraction

The development of an extraction sequence applied to the secondary mineralogy of the studied tailings is reported in detail by Dold (1999, 2001a,b). In a first phase of the study, a slightly modified six-step sequential extraction (“sequence A”) after Sondag (1981) and Tessier et al. (1979) was utilized: (1) 1 M NH_4 acetate, pH 4.5, 2 h; (2) 0.1 M Na acetate, pH 5, 2 h; (3) 0.25 M hydroxylamine–HCl, pH 2, 2 h; (4) 0.1 M oxalic acid, pH 3.3, heat, 1 h; (5) H_2O_2 35%, heat 1 h; (6) HNO_3, HF, $HClO_4$, HCl. The extractions were applied to drill core H1 in order to acquire information regarding the element distribution and the presence of possible secondary phases. In a second phase of the study, the sequence was modified to seven steps (“sequence B”; Dold 2001a,b) and adapted to the secondary mineralogy of the studied tailings (Table 1).

5.4. Acid–base accounting (ABA)

S_{total} content was measured using a Leco® furnace. For measurement of the $S_{sulfate}$, the 0.2 M NH_4 oxalate, pH 3.0, 80 °C, 2 h leach was used to dissolve

Table 1
Sequential extraction “B” applied in this study

Leach	Preferentially dissolved minerals	Refs.
(1) Water-soluble fraction 1.0 g sample into 50 ml deionized H_2O shake for 1 h	secondary sulfates, e.g., bonattite, chalcanthite, gy, pickeringite, magnesioauberite	Dold (1999, 2001a,b), Ribet et al. (1995), Fanfani et al. (1997)
(2) Exchangeable fraction 1 M NH_4 acetate pH 4.5 shake for 2 h	ca, vermiculite-type mixed layer, adsorbed and exchangeable ions	Dold and Fontboté (2001), Gatehouse et al. (1977), Sondag (1981), Fonseca and Martin (1986)
(3) Fe(III) oxyhydroxides 0.2 M NH_4 oxalate pH 3.0 shake for 1 h in darkness	sh, two-line fh, secondary jt, MnO_2	Schwertmann (1964), Stone (1987), Dold (1999, 2001b)
(4) Fe(III) oxides 0.2 M NH_4 oxalate pH 3.0 heat in water bath 80 °C for 2 h	gt, jt, Na-jt, hm, mt, higher ordered fh’s (e.g., six-line fh)	Dold (1999, 2001a,b)
(5) Organics and secondary Cu sulfides 35% H_2O_2 heat in water bath for 1 h	organics , cv, cc-dg	Sondag (1981), Dold and Fontboté (2001)
(6) Primary sulfides: combination of $KClO_3$ and HCl, followed by 4 M HNO_3 boiling	py, cp, bn, sl, gn, mb, tt, cb, op, stb	Chao and Sanzolone (1977), Hall et al. (1996)
(7) Residual HNO_3, HF, $HClO_4$, HCL digestion	Silicates, residual	Hall et al. (1996), Dold et al. (1996)

bn: bornite; ca: calcite; cb: cinnabar; cc: chalcocite; cv: covellite; cp: chalcopyrite; dg: digenite; fh: ferrihydrite; gn: galena; gt: goethite; gy: gypsum; hm: hematite; ilm: ilmenite; jt: jarosite; Na-jt: natrojarosite; mb: molybdenite; mt: magnetite; op: orpiment; py: pyrite; sh: schwertmannite; sl: sphalerite; stb: stibnite; tn: tennantite; tt: tetrahedrite.

all sulfates, such as jarosite, schwertmannite and gypsum (Dold, 1999, 2001a,b). Sulfur in the leachate was determined by ICP-AES. The differences of both results represent the $S_{sulfide}$ content. Total and mineral carbon was analyzed by coulometric titration (Ströhlein CS 702®). The sulfide net neutralization potential (SNNP) was calculated in $t CaCO_3/1000t$, with the assumption that at neutral pH, 4 mol of calcite (HCO_3^- dominant species at pH 7) are necessary for the neutralization of 4 mol H^+ produced by the oxidation of 1 mol of pyrite.

6. Results

6.1. Ojancos tailings impoundment no. 2

The Ojancos tailings impoundment no. 2 consists of a mixed stratigraphy of carbonate-rich material from the Teresita mine with high neutralization potential and low-carbonate material from the Las Pintadas district with high acid potential. In order to illustrate the element mobilization and retention pathway subsequent to sulfide oxidation, the results are presented following the present water flowpath, i.e., in the following order: (1) recent discharge point (pH 11), (2) AMD effluents (pH 3.15) at the lower part of the recent coarse tailings "2H" and (3) the "old" impoundment no. 2, including a primary zone recently flushed down from the "2H" tailings and deposited on the top of the old tailings impoundment no. 2 (pH 7), and the formation of the cemented zone (pH 4).

6.1.1. Mineralogy and acid–base accounting of sample HPr from the recent discharge point for tailings "2H"

The tailings at the present discharge point (HPr) for the tailings "2H," with a pH 11 (Fig. 2), consist mainly of quartz, alkali feldspar (mainly albite), calcite, Ca-amphibole (magnesio-hornblende), pyroxene (hedenbergite), magnetite, hematite, pyrite and minor chalcopyrite and micas (biotite and muscovite). These minerals belong to typical ore and alteration mineral assemblages in areas near the batholith (Marschik and Fontboté, 1996, 2001a). According to available information, the source of the "2H" tailings is the Las Pintadas district, close to the batholith, and the carbonate-hosted Teresita mine. The presence of Ca-amphibole in the sample HPr suggests that at the moment of sampling the discharge derivated from the Pintadas district.

The ABA of sample HPr shows a pyrite content of 3.5 and 7.1 wt.% calcite equivalent, resulting in a negative sulfide net neutralization potential (SNNP = −47.3 $t CaCO_3/1000t$). Other parts of the "2H" tailings, due to their provenance from the carbonate-hosted Teresita mine, must have high NP, so that an inhomogene distribution of AP and NP characterizes the "2H" tailings.

6.1.2. AMD effluents at the lower part of the recent deposited "2H" tailings

In November 1997, a small part of the "2H" tailings, directly at the contact with the old tailings impoundment no. 2, was flushed down by exceptional strong rainfalls in the Copiapó valley. This led to the outflow of acid effluents with the formation of orange-brown, pale blue, yellow and reddish precipitates (Fig. 3B). Three outflows were located within a small area of 50 cm diameter. The center effluent had a pH of 3.15 with orange-brown colored precipitates. XRD patterns show typical features for schwertmannite ($Fe_8O_8(OH)_6SO_4$, with broad peaks at 1.51, 1.66, 2.28, 2.55, 3.39 and 4.86 Å) and gypsum. A SEM image shows characteristic spherical forms of schwertmannite, 1–1.5 μm in size, and EDS analysis reflect high iron content (Fig. 4A). The other two outflows had pale blue precipitates and pH values of 4.90. XRD patterns with broad peaks at 4.25 and 8.5 Å as well as SEM-EDS data indicate that the precipitate is mainly chalcoalumite ($CuAl_4(SO_4)(OH)_{12}\cdot 3H_2O$). The SEM image (Fig. 4B) shows very fine particles (< 1 μm). At the confluence of the three effluents, the pH was 4.54, the color changed to pale yellow, and the XRD detected mineral is gypsum. The fact that two geochemically so different effluents discharge only 20 cm apart indicates that different geochemical conditions may coexist in close vicinity in the tailings material.

A water sample HWS was taken in 1996 from the small surficial pond of impoundment no. 2 (Fig. 2), which received surface seepage from "2H." Its high sulfate and metal concentrations (Table 2) have its origin in sulfide oxidation, the high Ca and Sr concentrations are interpreted to be liberated by acid neutralization with calcite and/or gypsum dissolution; the high Na concentrations may have its origin in the

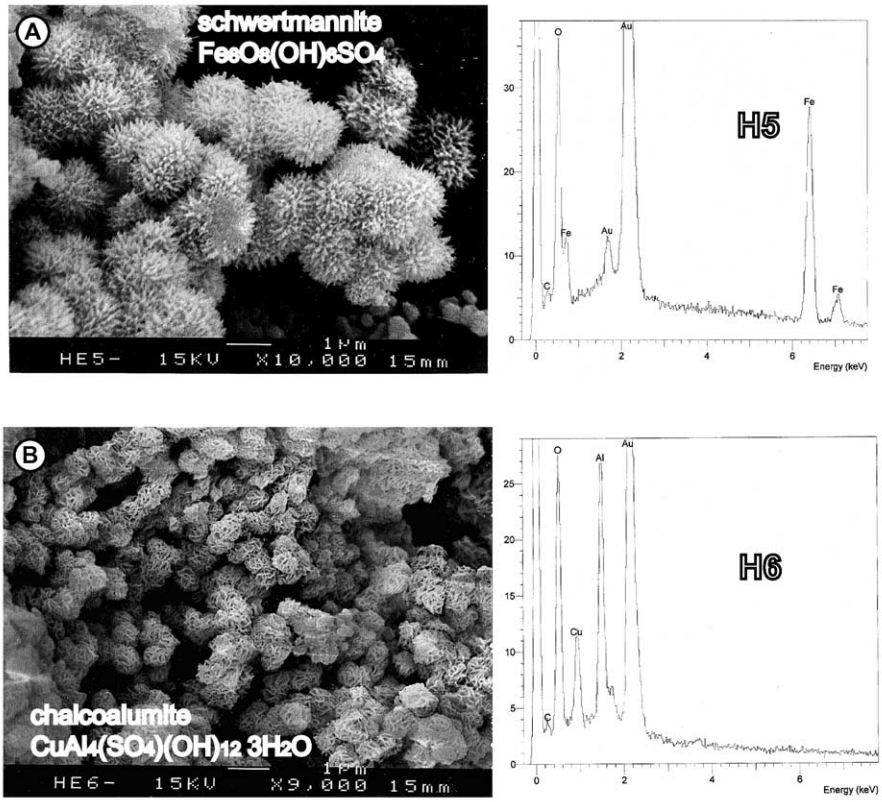

Fig. 4. (A) SEM photograph of sample HE5 with EDS spectrogram of schwertmannite, showing the typical spherical sea urchin reminding morphology. (B) SEM photograph with EDS of chalcoalumite (sample HE6).

application of Isopropil Na-Xantate, a commonly applied collector in the flotation process.

6.1.3. Stratigraphy, mineralogy and acid–base accounting of the Ojancos tailings impoundment no. 2

The stratigraphy is throughout the whole impoundment similar and characterized from the top to 10-m depth by the following succession: (1) about 3-m thick recent dark gray primary zone with paste pH 7 (being flushed down from the recent discharge point HPr at the uphill "2H" tailings), (2) about 3-m thick oxidation zone (pH 7) characterized by dark gray colored unoxidized coarser horizons intercalated by reddish brown (Fe(III)hydroxide-rich) fine-grained oxidized horizons and (3) a homogeneous, reddish brown cementation zone (pH 4) of which only about 2 m could be penetrated (Fig. 2). A general dipping of the recognized zones and of the ground water level towards the dam can be observed (e.g., ground water level at S8 = 1.2 m and S1 = 3.6 m). The stratigraphy,

Table 2
Water analysis of the surficial water pond (HWS) of the Ojancos impoundment no. 2

Field parameters		Anions (mg/l)		Major cations (mg/l)		Metal cations (mg/l)	
pH	7.55	SO_4	2836	Ca	786	Cu	0.12
T (°C)	9.2	Cl	3190	Mg	101	Mo	0.05
Conductivity (mS/cm)	13.61	HCO_3	109	Na	2350	Mn	0.36
O_2 (mg/l)	6.7	B	7.2	K	70	Sr	4.6
		F	1			Ba	0.04
		SiO_2	15			Li	0.15

mineralogy and geochemistry of the Ojancos tailings impoundment no. 2 is discussed in detail using the representative core H1 (Figs. 8 and 10), which was sampled in 1996 to 10-m depth near core S8 (from the 1994 campaign). Core H1 shows the same stratigraphy as S8 but the recent primary zone on the top of the profile reaches a depth of 2.8 m, instead the 1.3 m found in S8. This indicates that in the 2 years between the coring H1 and S8, 1.5 m of additional tailings material was flushed down from the uphill "2H" tailings. A change in grain size from fine sandy–silty ($K = 1 \times 10^{-7}$–3×10^{-7} m/s) in the primary and oxidation zones to clayey ($K = 3 \times 10^{-8}$–4×10^{-8} m/s) in the cementation zone is observed. The moisture content graded from 15 wt.% in the primary zone to 25 wt.% in the oxidation zone and to 33 wt.% in the cementation zone.

By a careful mineralogical study the tailings stratigraphy can be separated into three intervals, which are distinguished on the basis of their primary silicate and carbonate mineralogy (Fig. 5). The first interval corresponds to the recent primary zone being flushed

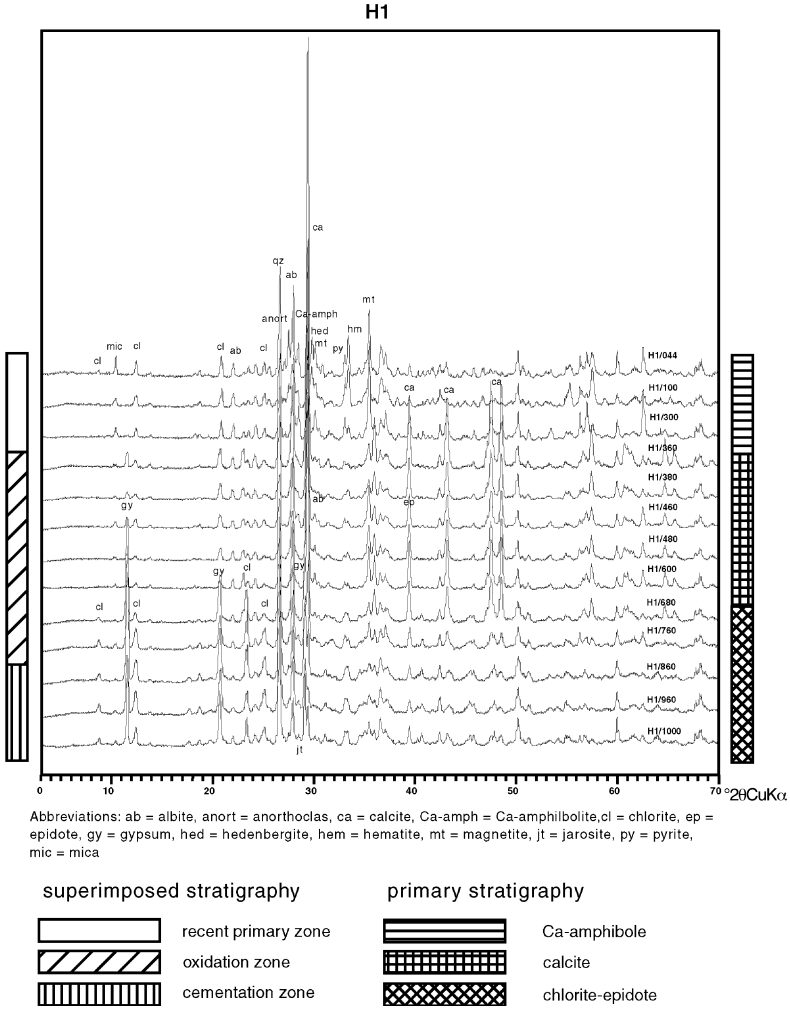

Fig. 5. Results of XRD from drill core H1 from the Ojancos impoundment no. 2. The stratigraphy and the proposed primary source of the tailings are shown.

down from the hillside "2H" impoundment and reaches to a depth of 2.8 m, which is dominated by quartz, alkali feldspar (mainly albite), Ca-amphibole (magnesiohornblende), pyroxene (hedenbergite), magnetite, hematite, pyrite (Fig. 3F) and minor chalcopyrite, calcite and micas (biotite). This mineral assemblage is very similar to that of the recent discharge point (sample HPr) and is also thought to derive from the Pintadas district (Fig. 1). Below, an interval from 2.8- to 7-m depth is characterized by abundant calcite and minor quartz, albite, magnetite and low pyrite, hematite and mica contents. The source for this carbonate-rich zone may be the Teresita mine or another calcite-rich mine. Below 7 m, the assemblage is dominated by quartz–albite–calcite–chlorite ± epidote, suggesting that this material may come from a mine in the eastern part of the Punta del Cobre belt (Marschik and Fontboté, 1996).

The sections of the primary stratigraphy are superimposed by a secondary zonation resulting from weathering processes. Below the recent primary zone, an oxidation zone follows between 2.8 and 8 m. This oxidation zone is characterized by the interlayering of coarser dark gray unoxidized layers with fine-grained, Fe(III) hydroxide-rich, ochre to red-brown colored horizons. The oxidation zone is calcite-rich with neutral pH values, which decrease in the lower part of the oxidation zone. The features of this oxidation zone are very similar to those found in the also carbonate-rich oxidation zone of the P. Cerda impoundments (Fig. 3C) and may be explained as follows: high evaporation in arid climates favors upward migration via capillary force (Dold and Fontboté, 2001) and limits sulfide oxidation to fine-grained horizons due to their higher water retention capacity. Generally, fine horizons are poorer in sulfides than coarser layers because of gravity separation during deposition, so that lower sulfide contents are available for oxidation. The mobility of the liberated elements is very low due to the neutral pH values so that secondary Fe(III) hydroxides precipitate in situ in the fine horizons, where the main sulfide oxidation takes place. This leads to a specific layering for oxidation zones of carbonate-rich tailings in arid climates.

The oxidation zone at the Ojancos impoundment no. 2 formed in the 10 years without operation (1977–1987) before the recent uphill deposition of the "2H" tailings and the flush down of the recent primary zone

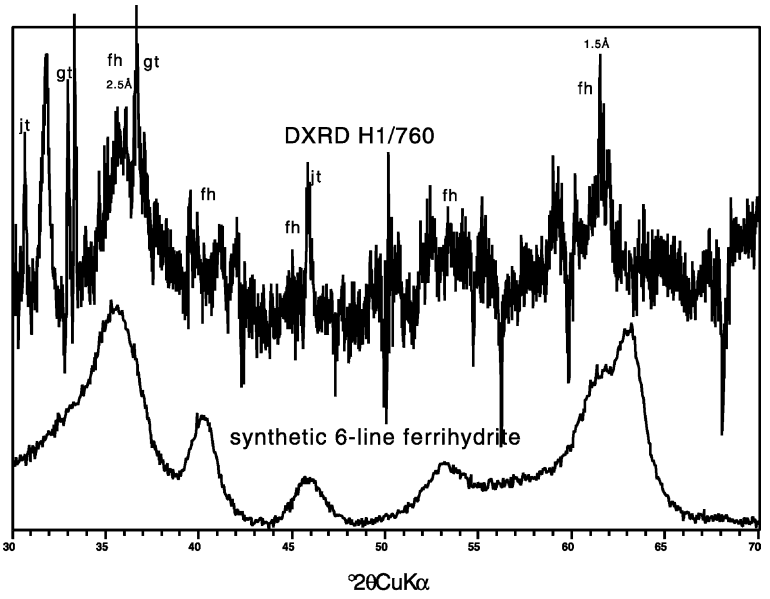

Fig. 6. DXRD of higher ordered ferrihydrite (five-line) with goethite and minor jarosite of the sample H1/760 of the cementation zone from Ojancos impoundment no. 2. For comparison, a diffractogram of a synthetic six-line ferrihydrite is shown.

at the top of impoundment no. 2. It is important to mention here that this oxidation zone, characterized by neutral pH because of the combination of high calcite and low pyrite content, can not be the source of the element enrichment found in the lower part of the oxidation zone and the underlying cementation zone. In the Ojancos no. 2 tailings, below the oxidation zone and down to the end of the drill holes (8–10 m), a cementation zone occurs with gypsum as the dominant phase (~ 9 wt.% gypsum equivalent). Subordinate five- and six-line ferrihydrite (~ 4–5 wt.% $Fe(OH)_{3(S)}$ equivalent) together with goethite and locally minor jarosite could be detected by DXRD (Fig. 6). The cemented zone is interpreted as a result of the seepage of acid solutions from the uphill "2H" tailings into the downstream impoundment. There, the hydrolysis of the secondary ferric phases (e.g., ferrihydrite, goethite) may be initiated by pH increase, for example, due to carbonate-rich layers. Higher ordering of the five- to six-line ferrihydrite (detected by DXRD, Fig. 6), presumed to form because of formation by slow hydrolysis (Schwertmann et al., 1999) and is in contrast to the normally lower ordered ferrihydrites (two- to four-line) encountered in acid mine drainage environment (Nordstrom and Alpers, 1999). Relictic pyrite, magnetite and hematite are very minor phases and secondary covellite can be observed in the cementation zone as fine disseminated grains (Fig. 3H). The low sulfide contents in the cementation zone can be explained because of oxidation by Fe(III). Oxidation of one mole of pyrite via ferric iron (Eq. (1)) has faster kinetics (Moses et al., 1987) and produces 16 mol of protons what is eight times more than via oxidation by oxygen (Eq. (2)). However, this is only the case when the ferric iron is added to the system, as it may be the case of the seepage of Fe(III)-rich solutions from the recent "2H" tailings or through dissolution of ferric minerals (Cornell and Schwertmann, 1996; Samson and Eggleston, 2000). If the ferric iron of Eq. (1) had to be produced within the tailings impoundment no. 2 by oxidation from ferrous iron (Eq. (3)), which is a proton consuming process, the net produced acidity during the oxidation of one mole of pyrite is 2 mol of protons, i.e., the same as pyrite oxidation via oxygen (Eq. (2)). Thus, an input of ferric iron by AMD results in an acidity transfer to the downstream tailings and must be considered for acid–base accounting. Additionally, the dissolution of primary hematite (Eq. (4)) and magnetite (Eq. (5)) in the low-pH cementation zone (Fig. 3G and H) is a potential source of Fe(III).

$$FeS_2 + 14Fe^{3+} + 8H_2O \rightarrow 15Fe^{2+} + 2SO_4^{2-} + 16H^+ \quad (1)$$

$$FeS_2 + \frac{7}{2}O_2 + H_2O \rightarrow Fe^{2+} + 2SO_4^{2-} + 2H^+ \quad (2)$$

$$Fe^{2+} + \frac{1}{4}O_2 + H^+ \Leftrightarrow Fe^{3+} + \frac{1}{2}H_2O \quad (3)$$

$$Fe_2O_3 + 6H^+ \rightarrow 2Fe^{3+} + 3H_2O \quad (4)$$

$$Fe^{2+}Fe_2^{3+}O_4 + 8H^+ \rightarrow Fe^{2+} + 2Fe^{3+} + 4H_2O \quad (5)$$

The calcite content decreases in the lower part of the oxidation zone, and calcite is completely absent in the cementation zone. The pH also decreases from values around 7 down to 5 in the lower part of the oxidation zone and is buffered in the cementation zone possibly by ferrihydrite to values around 4. The deepest sample H1/1000 (depth 10 m) shows again XRD detectable calcite and a pH value of 6. This may indicate that a calcite-rich horizon induced the formation of the cemented zone.

Calculation with the assumption that all sulfide sulfur is associated with pyrite results in pyrite contents of 3.5–4.8 wt.% in the recent primary zone, 1.5–2.9 wt.% in the oxidation zone and 1–1.8 wt.% in the cementation zone. The tailings of the primary zone have a SNNP of −83.4 to −158.5 $t CaCO_3/1000t$. In the oxidation zone, the SNNP is positive (14.4–417.8 $t CaCO_3/1000t$). This is consistent with the abundant calcite (up to 47 wt.%) and low pyrite contents. Below the oxidation zone, and in spite of low sulfide content, the ABA becomes negative again due to the decrease of calcite abundance, possibly because of neutralization reactions with down-seeping acid solutions. Thus, the general stratigraphy of the Ojancos impoundment no. 2 is characterized by the presence of a neutralizing zone intercalated between two acid producing zones.

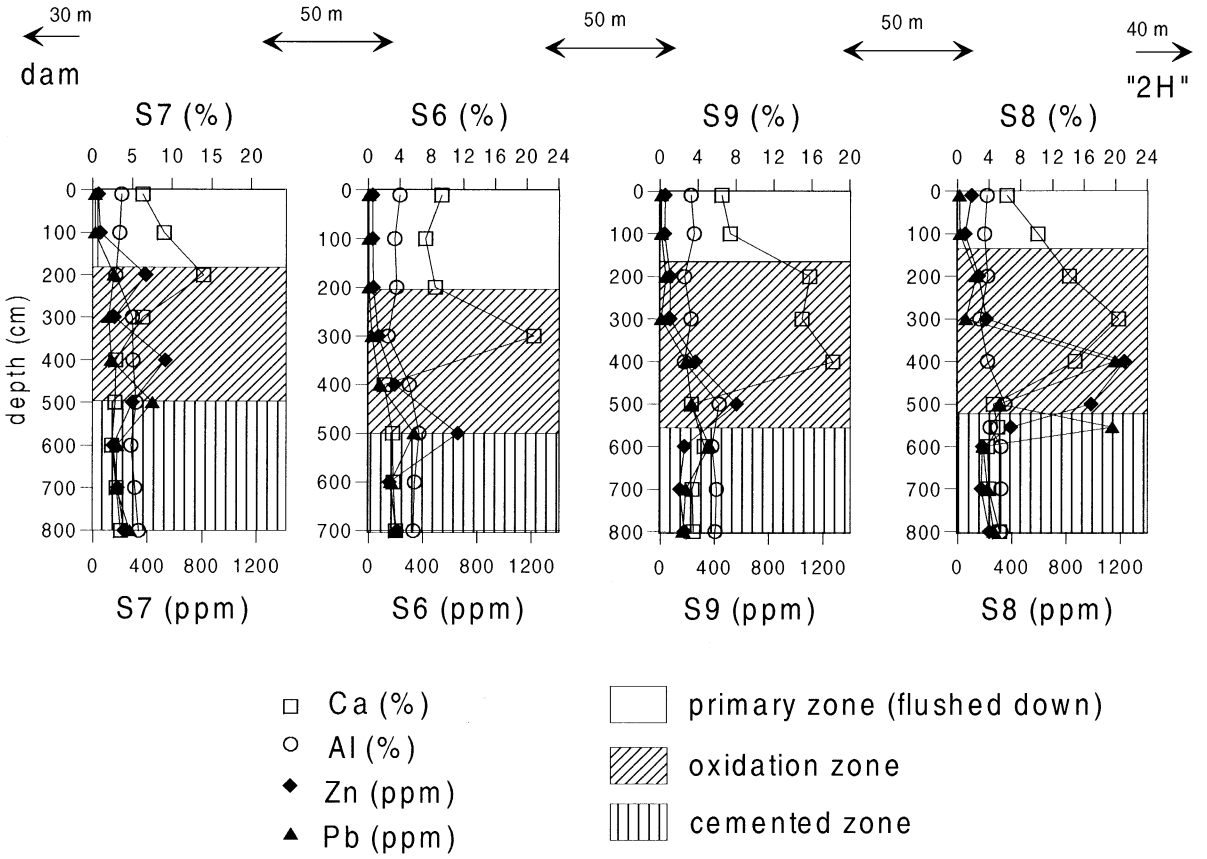

Fig. 7. Ca and Al as indicators for primary carbonate and silicate distribution in the drill cores S7, S6, S9 and S8. Zn and Pb concentrations show a peak located below the Ca peak (calcite) and above the cementation zone, indicating that the flow of metal reach solution is defined in between these two zones. Heavy metal concentrations are about three times higher near the seepage input (S8) than near the dam (S7).

6.1.4. Geochemical results

In the preliminary stage of this investigation, total digestion analyses were performed. The results from drill cores S1, S2, S3, S6, S7, S8 and S9 show maximum values of all heavy metals in an interval spanning the lower part of the calcite-rich oxidation zone and the upper part of the cementation zone (Fig. 7). The intensity of the heavy metal peaks decreases with increasing distance from the seepage input. As total digestion results give limited information about geochemical processes, they will not be discussed here in detail. Data are available in Dold (1999, Tables 2–5, Chap. 6), also accessible under Bernhard Dold's homepage at http://www-sst.unil.ch/perso_pages/index.htm.

Much more informative are analyses of sequential extractions. The results of sequential extractions of the representative drill core H1 (located close to S8) are shown in Fig. 8 and (six-step sequence A) and in Fig. 9 (seven-step sequence B for some selected samples). For better visibility of the geochemical fingerprints of secondary phases (e.g., jarosite), the residual fraction for some elements (e.g., Fe, K) are not presented in Figs. 8 and 9. The analytical results using extraction sequence A (Fig. 8) will be discussed in the following three groups: (1) K and the relatively immobile elements Ti and Al, that may be taken as indicators of the primary silicate minerals; (2) the elements Ca, Mn and Mg are indicators for the carbonate distribution; (3) constituents that show important concentra-

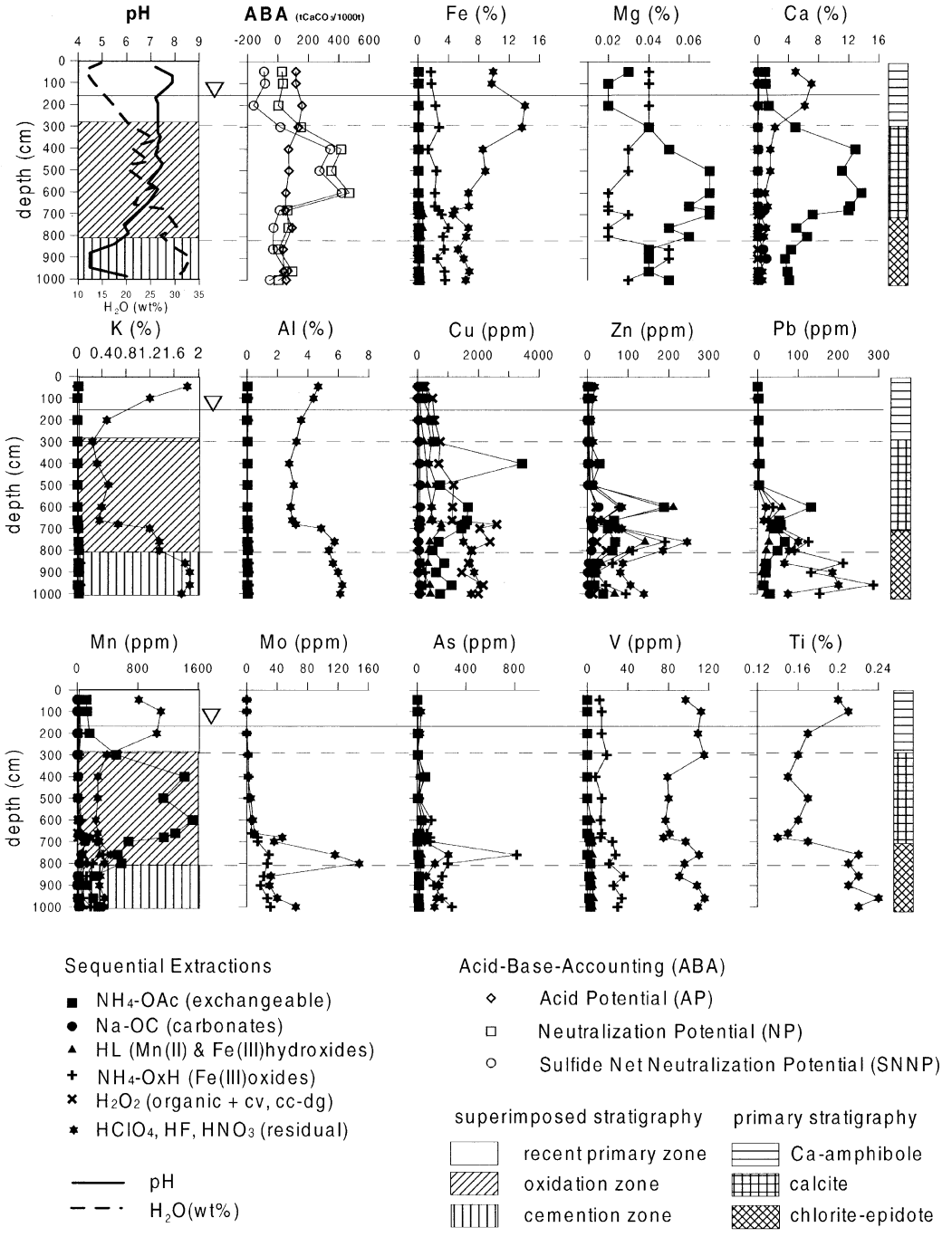

Fig. 8. Results of sequential extraction (sequence A) of drill core H1 from the Ojancos impoundment no. 2. Bulk results are not shown for better visibility of the data. All data are published in Dold (1999, Chap. 6) and under Bernhard Dold's homepage at http://www-sst.unil.ch/perso_pages/index.htm. This is also the case for Figs. 9, 11 and 12).

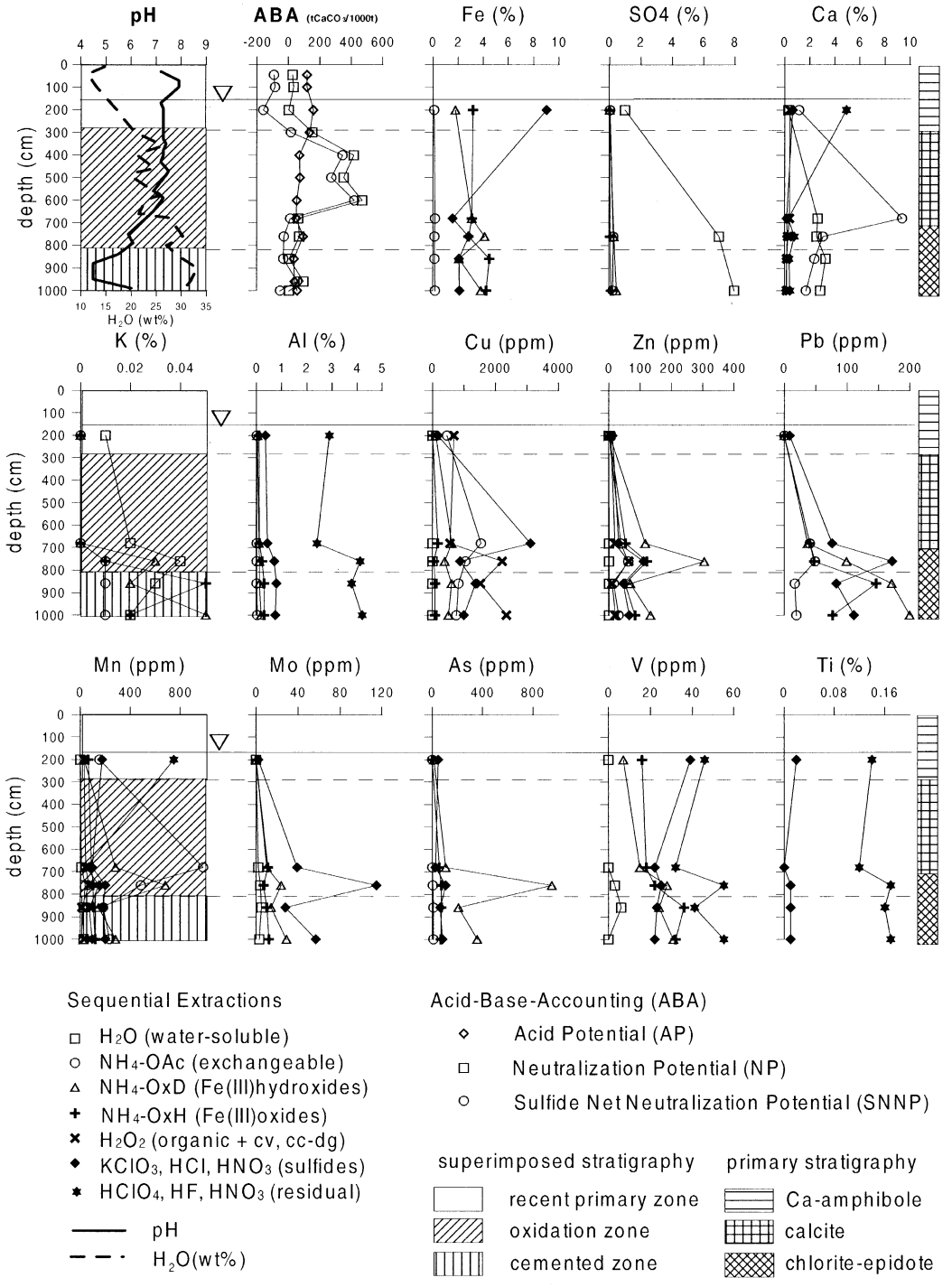

Fig. 9. Results of sequential extractions (sequence B) of selected samples from drill core H1 from the Ojancos impoundment no. 2.

tion variations in the oxidation and cementation zones (Fe, SO_4, Cu, Zn, Pb, Mo, As and V).

Three intervals can be distinguished according to their Ti, Al and K concentrations in the residual fraction. They coincide with those defined by mineralogical criteria. The upper part of the primary zone down to 2.8-m depth shows higher concentrations (Ti = 0.2%, Al = 4%, K = 1.2–1.8%) than in the following interval from 2.8- to 7-m depth (Ti = 0.16%, Al = 3%, K = 0.4%). Below 7-m depth, the concentrations are also higher than in the interval from 2.8 to 7 m (Ti = 0.2, Al = 5% and K = 1.6%). Results of the first four extraction steps of sequence B (Fig. 9) indicate that K increases in the cementation zone compared to the overlying oxidation and primary zones, indicating that K is available as a water-soluble and adsorbed cation, and possibly fixed in locally present jarosite as indicated by XRD and DXRD.

A similar stratigraphy is described by the Ca, Mn and Mg contents. In the residual fraction, Ca shows concentrations of about 6% in the upper 2.8 m, and values below 2% in all deeper samples. The Ca contents in the exchangeable fraction of sequence A (Fig. 8), in which gypsum is dissolved together with calcite, show low concentrations in the upper 2 m. In the section between 2.8- and 7-m depth, the Ca content increases up to 12% which is consistent with the abundant presence of calcite (XRD). Between 7 and 10 m, the exchangeable Ca contents are around 4%. In the lower part of the oxidation zone, calcite is scarce and in the cementation zone, it was not detected by XRD. Gypsum becomes a dominant phase in the cementation zone. Application of a water leach before the exchangeable leach (sequence B, Fig. 9), permits quantitative discrimination between gypsum and calcite and shows that most of the Ca is fixed in the water-soluble fraction as gypsum, confirming the XRD results. Mn follows the same distribution as Ca in the upper 7 m. At 7.5-m depth, Mn shows a peak in the fraction of the Fe(III) hydroxides (Fig. 9), which may indicate the dissolution of secondary Mn(II) hydroxides. Mg shows a similar distribution as Ca and Mn in the exchangeable fraction, indicating that the gangue carbonates are at least in part Mg-and Mn-bearing calcites, which is typical for hydrothermal Fe oxide Cu–Au systems (e.g., calcite from Punta del Cobre: 0.02% and 0.03% Mg and 3240 and 6790 ppm Mn; Candelaria: 0.03% Mg und 1440 ppm Mn; Marschik, 2002; personal communication). The distribution of these elements confirms the mineralogical stratification of the primary tailings composition described above.

Fe, SO_4, Cu, Zn, Pb, Mo, As and V show important concentration increases in the lower part of the oxidation zone and in the cementation zone (Fig. 8 and 10). This is explained by the precipitation of secondary sulfates, ferric hydroxide phases and secondary sulfides, as well by strong adsorption of mobile heavy metals. The precipitation of secondary ferrihydrite, goethite and jarosite in the lower part of the oxidation zone and the cementation zone is reflected in the increase of Fe concentrations in the Fe(III) oxides fraction. The strong enrichment of bivalent cations such as Cu (up to 0.65%), Zn (up to 600 ppm) and Pb (up to 500 ppm) compared to values in the primary zone of about Cu (0.2%), Zn (20 ppm) and Pb (13 ppm), respectively, is mainly associated with the layers below the calcite-rich tailings, where low pH (about 4) ensures the mobility of these metals. At pH values below 6, Cu precipitates mainly as covellite, whereas above pH 6, in the vicinity of the calcite-rich parts of the oxidation zone, adsorption dominates as shown in the increase in the exchangeable fraction. This pH dependence of the secondary Cu sulfide formation is also recognized in porphyry copper tailings (Dold and Fontboté, 2001). Zn shows a concentration maximum at the top of the cementation zone mainly in the fraction of the Fe(III) hydroxides (Fig. 9). The adsorption of Zn on ferric hydroxides is pH-controlled and requires pH values of 5 or higher (Dzombak and Morel, 1990; Webster et al., 1998). This explains why, in the low-pH cementation zone, less Zn is associated with the ferric hydroxides than in the lower part of the oxidation zone, where the pH reaches 6. Pb adsorbs on ferric hydroxides at pH values greater than about 3.5 (Dzombak and Morel, 1990; Webster et al., 1998), which is reflected in high Pb concentrations of the Fe(III) hydroxide and Fe(III) oxide fractions over the whole cementation zone.

The oxyanions Mo, As and V show also peaks at in the lowest part of the oxidation zone and increased values in the cementation zone compared to the upper parts of the drill core (Figs. 8 and 9). These elements have a high affinity to ferric hydroxides under acid conditions (Dzombak and Morel, 1990). Arsenic is

mainly associated with the easily reducible Fe(III) hydroxide fraction in the cementation zone. Vanadium enrichments are associated to the water-soluble, Fe(III) hydroxide and Fe(III) oxide fractions (Fig. 9). Vanadium is the only heavy metal available in relevant amounts in the water-soluble fraction in the cementation zone. This may be explained by its complex geochemical speciation. Under oxidizing

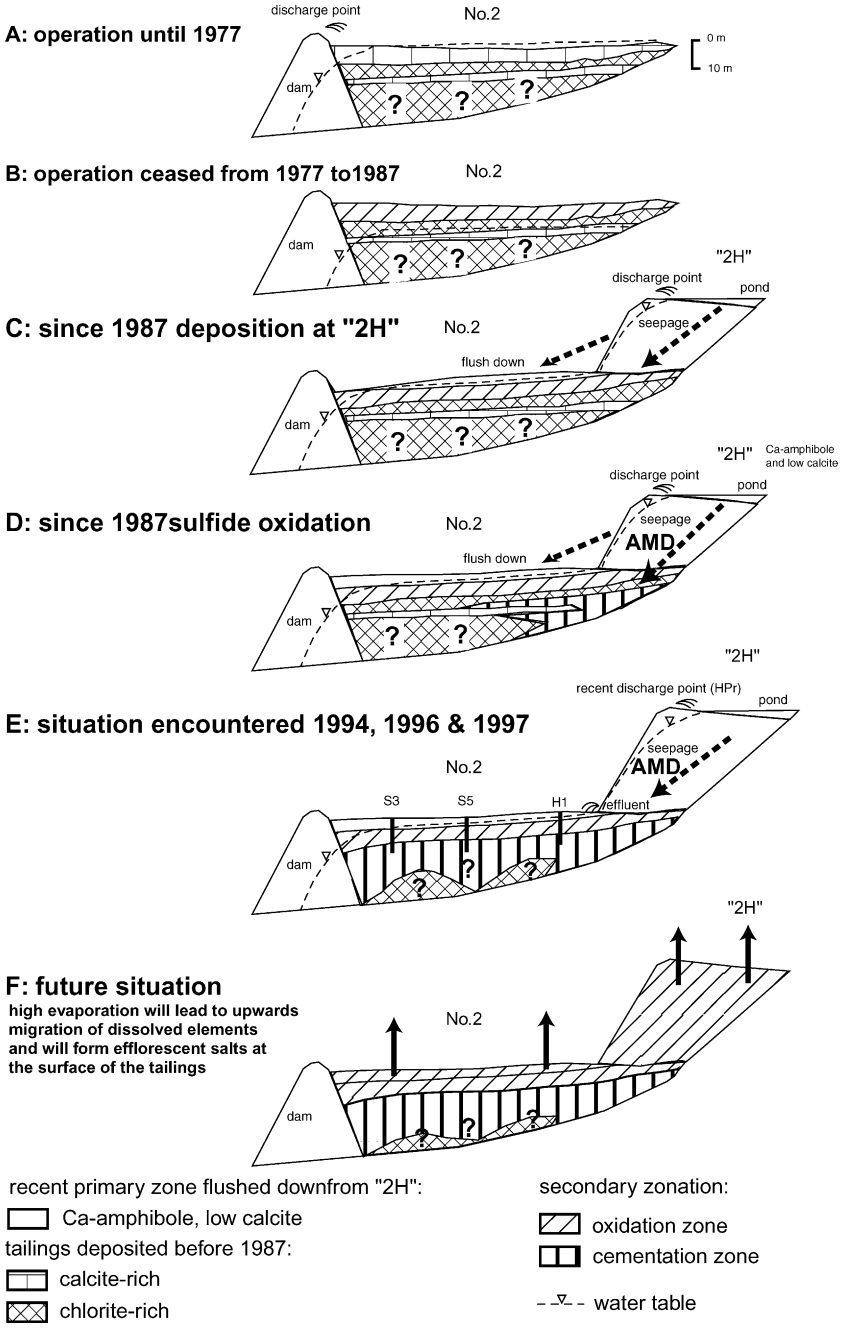

conditions V is stable as $H_2VO_4^-$ in the pH range between 2 and 8. Under reducing conditions, it is stable as VO^{2+} up to pH values of 5 (Brookins, 1988). $H_2VO_4^-$ is possibly adsorbed under acid conditions at ferric polymers. The polymerization of ferric ions is reviewed by Schwertmann et al. (1999). A polymer is defined as a continuum of aqueous ferric complexes with more than one iron atom and including the colloidal size fraction. With their outstanding reactive OH^- groups, they can play an important role in the sorption of ions and the colloidal transport (Andersson et al., 2001; Chen et al., 2001; Ren et al., 2001). Due to the high water input at the active "2H" tailings, the ferric polymers may migrate downward and transfer the adsorbed V to areas under reducing conditions, where it will be available as water-soluble cation VO^{2+} in the low pH cementation zone. Mo shows its highest concentrations in the sulfide leach in the lowest part of the oxidation zone (Fig. 9). This is interpreted as secondary Mo sulfide precipitation under the slightly reducing conditions below the water level (Brookins, 1988).

The Ojancos site shows that the mainly negative ABA, in combination with the coarse grain size and the high water input of the recently deposited "2H" tailings, lead to the formation of AMD, which seeps in the older tailings impoundment. There, where the acid solution reaches carbonate-rich horizons (+ABA), hydrolysis of ferric hydroxides will be initiated and the formation of a cemented zone starts leading to enrichment of the mobilized metals. Low pH conditions in the cemented zone (pH 4) ensures the mobility of Cu and enables so the secondary Cu sulfide (covellite) precipitation under more reducing conditions. A model of the development of the stratigraphy found in the Ojancos no. 2 impoundment is summarized in Fig. 10.

6.2. Tailings impoundments nos. 4 and 6 of the Pedro A. Cerda treatment plant, Fe oxide Cu–Au deposit Ojos del Salado, Tierra Amarilla, south of Copiapó, northern Chile

6.2.1. Physical properties and mineralogy P. Cerda tailings impoundments nos. 4 and 6

The four cores obtained from tailings impoundments nos. 4 and 6 from the P. Cerda flotation plant reached a maximum depth of 5.9 m. The paste pH in all core samples remained in the neutral range (6.9–8.3). Calcite content amounts to about 10 wt.% and pyrite up to 2.5 wt.%. The younger upstream impoundment no. 6 has an oxidation zone at the top with 5-m thickness in drill core O1 and 3.6 m in drill core O2 (Fig. 2). The oxidation zone is similar to that of Ojancos impoundment no. 2 and shows alternating coarse grain-sized horizons without macroscopic indication of oxidation and fine-grained horizons of ochre to reddish brown color indicating the precipitation of secondary Fe(III) hydroxides (Fig. 3C). Below the oxidized zone, there is a dark gray colored primary zone. The moisture content increases in core O1 from 2.7 wt.% at the top to maximum values of 22.2 wt.% at depth. In core O2, near the dam, the maximum moisture content is 5.2 wt.%.

The gangue mineralogy in the uphill impoundment no. 6 is homogeneous. With decreasing abundance, the main minerals are quartz, chlorite, calcite, albite-±anorthoclase, magnetite, hematite, epidote and gyp-

Fig. 10. Proposed model to explain the stratigraphy found in the Ojancos tailings impoundment no.2. (A) Until 1977, the Ojancos treatment plant bought the ore from different mines in the Punta del Cobre belt, leading to an interlayering of carbonate-rich and carbonate-poor layers. During operation, the impoundment was water saturated and no oxidation took place. (B) In 1977–1987, the operation ceased at the impoundment no. 2 and an oxidation zone in the calcite-rich upper part was formed. (C) In 1987, the recent deposition at "2H" started, resulting in the coeval flush-down of primary tailings over the old oxidation zone. (D) Simultaneously, sulfide oxidation took place at "2H" and AMD started to seep into the impoundment no. 2. Acid metal loaded solutions were neutralized at horizons with high calcite content, hydrolysis of ferric phases is initiated and the formation of a cementation zone could start. With time, this low-permeability cementation zone changed the downwards water flow to a lateral flowpath on the top of the cementation zone, leading to heavy metal enrichment in and directly above the cementation zone. (E) The situation encountered during the sampling period shows that the cementation zone can be observed in the whole impoundment. It is not clear if the whole underlying material is cemented or primary material is still remaining. (F) The operation stopped 1998, under the prevailing extreme arid climate the migration direction will change to upwards, the recent primary zone will start to oxidize and due to the lower neutralization potential in the primary zone and in "2H" possibly low-pH conditions will develop, leading to the formation of efflorescent salts at the top of the tailings.

sum. The chlorite–epidote assemblage is an indicator for the alteration in the eastern part of the Punta del Cobre belt. Polished sections reveal that in the coarse pyrite-rich horizons (due to gravity separation) the pyrite is mainly unoxidized, strongly fractured, and does not show oxidation rims or coatings. Whereas in fine grain-sized horizons, pyrite oxidation is visible by the presence of secondary Fe(III)hydroxides. The pyrite content varies strongly. Traces of chalcopyrite and very minor supergene replacement by chalcocite–digenite occur. Secondary covellite is detected as a trace constituent in the lower part of the primary zone. Magnetite is generally coarse-grained, in places partly altered to hematite. Most hematite occurs in form of mm-sized grains of specularite as described by Marschik (1996) and Marschik and Fontboté (2001a).

Drill core O4 at the older impoundment no. 4 shows a similar composition and the same interlayering as described for impoundment no. 6. Differences are the higher amounts of calcite and dolomite, and the smaller abundance of chlorite. The moisture content is also low with maximum values up to 7%, which is consistent with its location near the dam.

The stratigraphy of drill core O3, located at the foot of impoundment no. 6, shows an important difference. From the top to the bottom, the drill core intersects first a homogeneous gray–green primary zone interpreted to have flushed down from the impoundment no. 6. Below, an oxidation zone with Fe(III) hydroxide rich horizons follows to a depth of 1.8 m. Acid–base accountings show that the upper 2 m (flushed down primary zone and oxidation zone) have a negative SNNP (-75.9 $t CaCO_3/1000t$) indicating a significant acid producing potential of the primary zone, while the underlying, homogeneous reddish brown, silty–glayey ($K = 3.3 \times 10^{-8}$–3.6×10^{-8} m/s) cementation zone has a positive neutralizing potential (SNNP = 24.4 $t CaCO_3/1000t$). This reddish brown zone is similar to the cementation zone described in the Ojancos impoundment no. 2 before. The moisture content in O3 increases from zero at the top to a constant value of 23 wt.% in the cementation zone. The mineralogy in this part of the impoundment is dominated by quartz, albite ± anorthoclase, calcite, chlorite, magnetite, hematite, epidote, pyrite and minor gypsum. Relative to the oxidized zone, gypsum and calcite are abundant in the cementation zone (~ 4.3% and 9.2%, respectively). Polished sections show that in the cementation zone only some residual, very small pyrite grains remain. The reddish brown color suggests that ferrihydrite and goethite are present, but DXRD did not show conclusive results.

6.2.2. Geochemical results

Constant Ti values and XRD results of drill core O1 (uphill impoundment no. 6) indicate that the upper 5 m of the tailings are from similar primary composition, and derived from an ore with a calcite-rich gangue. Results from sequential extractions (Fig. 11, sequence A) show that the major elements Na, Fe, K, Ca and Mg are not significantly mobilized under the near neutral pH condition prevailing in the impoundment. However, metals which under oxidizing and acid to neutral conditions are stable as bivalent cations, such as Cu, Zn and Mn, show concentration decrease at the top of the oxidation zone and enrichments in the exchangeable fraction and in the fraction of the Fe(III) hydroxides in samples located below (Fig. 11). Cu shows a slight increase downward in the fraction of secondary copper sulfides (from 66 ppm at the top to 930 ppm at 5-m depth in the H_2O_2 leach), which is consistent with the presence of traces of secondary covellite. The oxyanions Mo and As show increasing values with depth mainly in the fraction of the Fe(III) hydroxides.

Results from sequential extractions (Fig. 12, sequence B) of drill core O3 (impoundment no. 4) show slightly decreasing Ti and Al concentrations in the primary zone of, suggesting a different origin of the upper part of the tailings, which is consistent with the hypothesis that they have flushed down from the younger impoundment no. 6. Fe, SO_4, Ca, Cu, Zn, Mn, Mo and As show increased concentrations in the cementation zone in the exchangeable fraction and the fraction of the Fe(III) hydroxides (Fig. 11). The high Fe, SO_4 and Ca concentrations are consistent with abundant gypsum observed by XRD and visible Fe(III) hydroxides. The high Mn concentration, mainly in the exchangeable fraction of the cementation zone, is interpreted as a result of calcite dissolution in this leach, similarly as discussed for Ojancos. The enrichment of the heavy metals Cu, Zn, Mo, as well as of As in the cementation zone is strongly associated to Fe(III) hydroxides and the exchangeable fraction, suggesting they are adsorbed to ferric polymers.

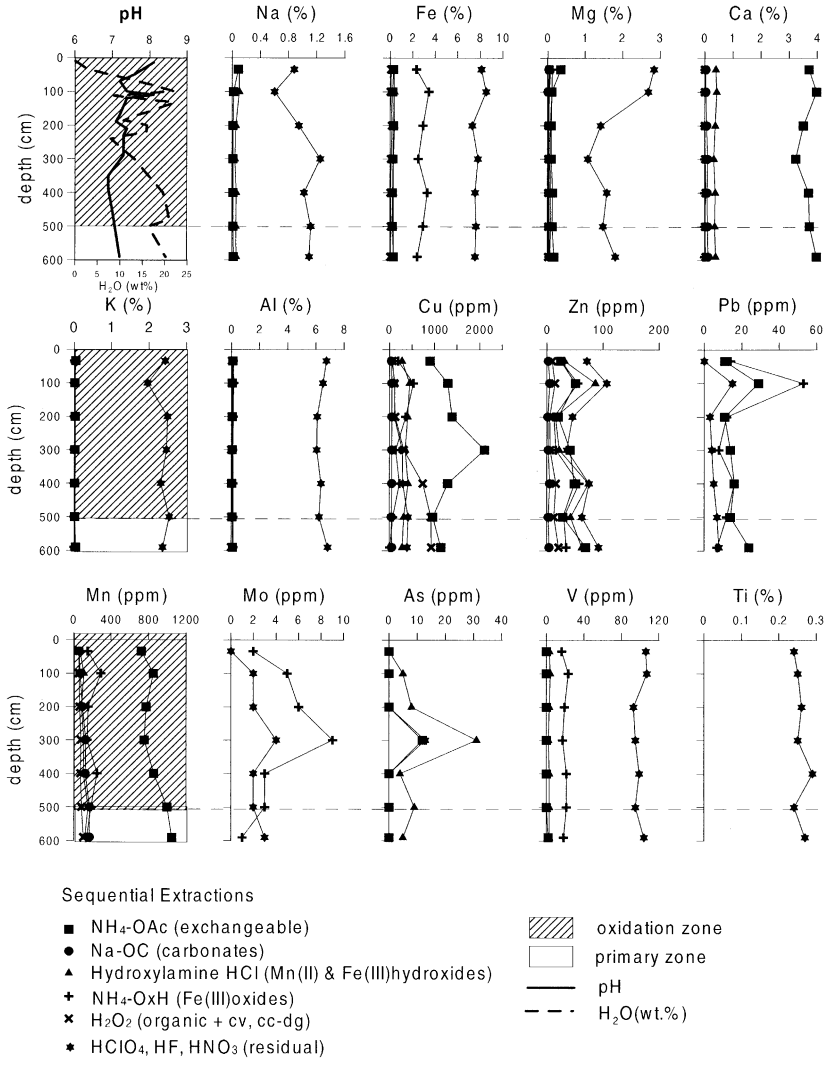

Fig. 11. Results of sequential extraction (sequence A) of drill core O1 from the P. Cerda impoundment no. 6.

6.2.3. Model of the development of the stratigraphy found in the P. Cerda impoundments

The neutralization potential of the P. Cerda tailings is high enough to maintain pH at neutral values. Pyrite oxidation takes place, as shown by the formation of an oxidation zone with precipitation of secondary Fe(III) hydroxides essentially in the fine-grained, relatively richer in moisture horizons, similarly as in Ojancos (Fig. 3C). In the coarser grain-sized horizons, where the main pyrite concentrations are found due to gravity separation, no visible pyrite oxidation takes place. This is attributed to the extreme arid climate, resulting in fast evaporation of the water in the coarser horizons after operation. Due to high water input during operation of the uphill impoundment no. 6, a constant water flow downstream is assumed, in a similar way as observed during sampling at Ojancos. Calcite distribution is homogeneous, whereas the pyrite content varies strongly, leading to locally strong differences in the ABA. Acidic, metal rich solutions may migrate and form "acid spots" or "channels" as shown by the Ojancos effluents, or if the pH is buffered to neutral,

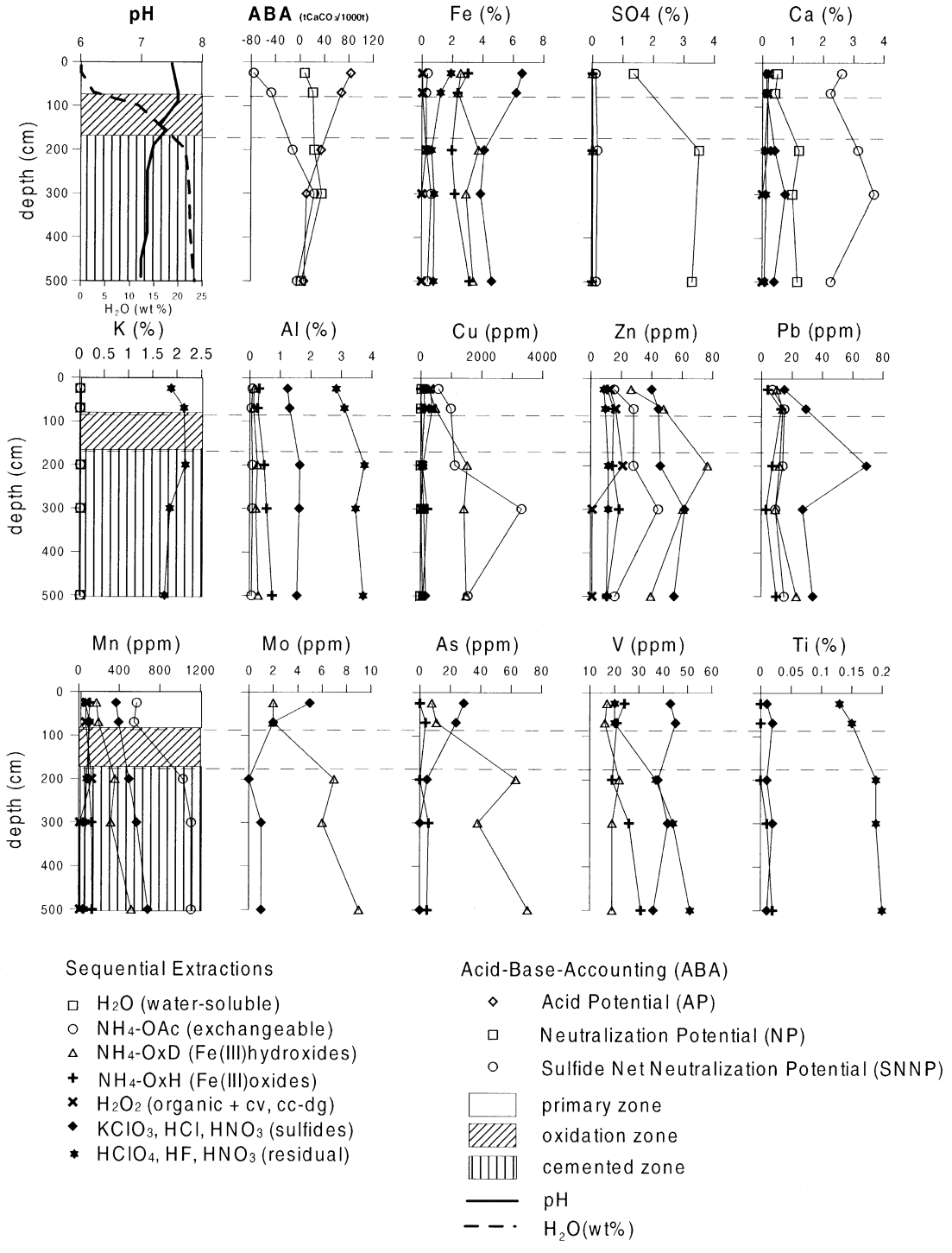

Fig. 12. Results of sequential extraction (sequence B) of drill core O3 from the P. Cerda impoundment no. 4.

ferric polymers will hydrolyze. An additional source of ferric iron may be the dissolution of magnetite and hematite by CO_3 complexation at neutral to alkaline pH conditions (Bruno et al., 1992; Hummel, 2000; Bruno and Duro, 2000). The neutral pH will have the effect that the liberated metal cations and anions will adsorb to the ferric polymers and may be transported downstream to the older impoundment no. 4. This would explain the metals enrichments in the cementation zone, which are mainly associated to the exchangeable fraction and not as secondary sulfides. If the transport would have taken place under acid conditions as dissolved ions, formation of secondary sulfides as, e.g., covellite should be encountered.

When operation of the mineral processing plant stopped, oxidation on the whole surface started and an unsaturated zone formed. In addition, by ceasing of water input, the downward metal mobilization stopped in this extreme arid climate. It can be assumed that in future the general migration direction will change to an upward transport by capillary force as reported by (Dold and Fontboté, 2001). The high carbonate content of the studied oxidation zone of the tailings impoundments of P. Cerda maintains the pH at a neutral level, favoring the adsorption of liberated elements, thereby decreasing their mobility. The suppression of upward migration of liberated elements during sulfide oxidation explains the total absence of secondary efflorescent salts at the top of the P. Cerda tailings impoundments.

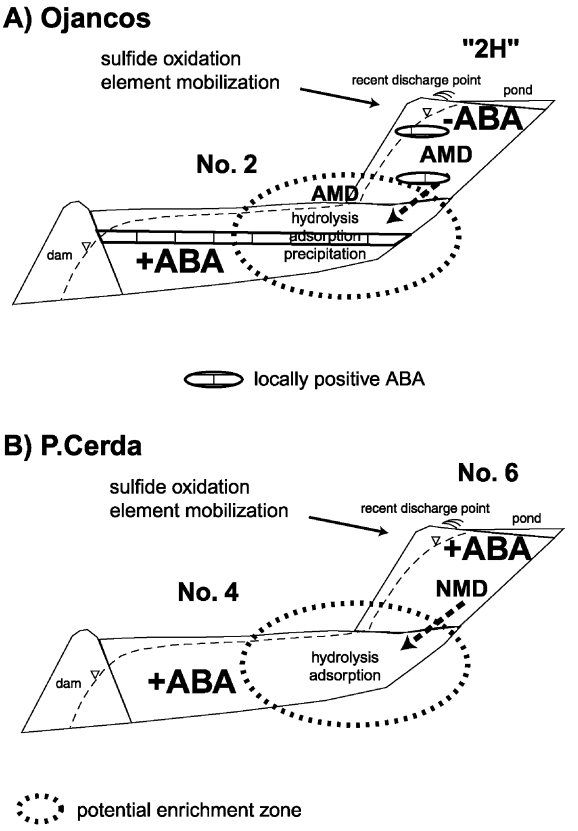

Fig. 13. Proposed model of influence of carbonate distribution and secondary enrichment processes as a result of impoundment construction with the potential enrichment zone.

7. Discussion

In this detailed geochemical and mineralogical study, two flotation tailings sites (Ojancos and P. Cerda) from the Fe oxide Cu–Au Punta del Cobre district, south of Copiapó, in the Atacama desert of northern Chile are compared (Fig. 13; Table 3). The application of sequential extraction in combination with detailed mineralogy allowed the reconstruction of the complex impoundment history and the source of the primary material at Ojancos. Both, at Ojancos and at P. Cerda, tailings filled valley dam impoundments (Fig. 13; mixed zonation with +ABA and −ABA at Ojancos and homogeneous +ABA at P. Cerda). After ceasing operation of the older impoundments new tailings were deposited upstream with −ABA (Ojancos) and +ABA (P. Cerda). This resulted in seepage migration from the upstream new tailings into the older tailings impoundment.

At Ojancos (Figs. 13A and 14A), where the recently deposited tailings (“2H”) have mainly an excess of acid potential (7.1 wt.% calcite and 3.5 wt.% pyrite), sulfide oxidation takes place at “2H,” with metal liberation and the production of acidity and the subsequent neutralization reactions. As the ABA of the “2H” tailings is negative, AMD can develop and the leach out of elements results in a significant mass transfer by acid seepage into the downstream no. 2 tailings. Out flows at the interface between the uphill and downhill tailings with the precipitation of schwertmannite (pH 3.15) and chalcoalumite (pH 4.9) confirms the AMD formation. The upper part of the no. 2. tailings consist of a recent primary zone

Table 3
Mineralogical characteristics of the oxidation and cementation zone of the tailings impoundments Ojancos no. 2 and P. Cerda no. 4

	Ojancos no. 2		P. Cerda no. 4	
	Primary	Secondary	Primary	Secondary
Oxidation zone	dark gray coarse horizons, mt (up to 10%) ± hm, ca-rich (~40 wt.%), py (1.5–2.9 wt.%)	Reddish brown to ochre horizons Fe(III) hydroxides (fh, gt),[a] pH 7	dark gray coarse horizons, mt (up to 10%) ± hm, ca-rich (~ 10 wt.%), py (~1 wt.%), chl-ep alteration	Reddish brown to ochre horizons Fe(III) hydroxides (fh, gt),[a] pH 7
Cementation zone	chl-ep alteration	Homogeneous reddish brown, five- to six-line fh, gt, jt, gy, dissolution of ca, mt and hm. $K = 3.2 \times 10^{-8} - 4.4 \times 10^{-8}$ m/s, < 1.7 wt.% py,[b] due to oxidation by Fe(III); pH 4	chl-ep alteration	Homogeneous reddish brown, fh,[a] gt,[a] gy, dissolution of ca, mt and hm. $K = 3.3 \times 10^{-8} - 3.6 \times 10^{-8}$ m/s, < 0.34 wt.% py, due to oxidation by Fe(III); pH 7

Abbreviation as in Table 1, chl = chlorite, ep = epidote, K = permeability.
[a] Indications but not unequivocally proved.
[b] The calculation is based on the S-sulfide content, but secondary sulfide precipitation (cv) in this zone suggests that the effective pyrite content is lower, supported by microscopic results.

(up to 3 m thick, pH = 7) with high acid potential (about 3 wt.% calcite and 4 wt.% pyrite). It buries an oxidation zone mainly characterized by unoxidized coarser horizons (sulfide, iron oxides and calcite are stable), with interlayering of fine-grained reddish brown horizons rich in secondary Fe(III)hydroxides. The high pH conditions in the recent primary and in the oxidation zone limit the element mobility. However, the upstream "2H" acid mine drainage extensively percolate through the no. 2 tailings and produce a >2-m (only 2 m penetrated by coring) thick low permeable cemented zone (pH = 4). This "hardpan" is essentially controlled by pH increase related to calcite-rich intercalations favoring the hydrolysis of the secondary ferric phases ferrihydrite, goethite and minor jarosite together with the precipitation of gypsum (Fig. 14A). The increase of pH because of the vicinity of intervals with high neutralization potential also raises the sorption of the metals transported by the acid seepage input and where more reducing conditions are encountered (below groundwater level) secondary sulfide precipitation leads to secondary Cu sulfide enrichment (covellite). This leads to a strong enrichment in the cementation zone (e.g., up to 6800 ppm Cu, 680 ppm Zn, 1100 ppm As). The fact that the cemented zone has very homogene low-pH conditions is interpreted as a result of the very effective acid transfer by input of Fe(III) from 2H to the older no. 2 impoundment, as pyrite oxidation by Fe(III) produces eight times the acidity as by oxidation via oxygen, resulting in a fast consummation of the neutralization potential (calcite dissolution). The established low-pH conditions, additionally can liberate Fe(III) through magnetite and hematite dissolution (Eqs. (4) and (5)) (Cornell and Schwertmann, 1996; Samson and Eggleston, 2000). The homogene pH 4 most likely is buffered by the dissolution equilibrium of the secondary ferric phases ferrihydrite and goethite. By comparison with studies on other tailings in the Atacama desert (Dold and Fontboté, 2001), it is hypothetized that in the future, when water input from the uphill impoundments definitely stops, the extreme arid conditions in combination of the – ABA of the primary zone will lead to capillary upwards migration and the formation of water-soluble sulfate minerals at the surface of the tailings, making metals available for remobilization with each rainfall.

In contrast, at P.Cerda (Figs. 13B and 14B), where the neutralization potential is homogeneously distributed in all tailings and generally exceeds the acid potential (average of about 10 wt.% calcite and maximal 2.5 wt.% pyrite), the paste pH values are 6.9–8.3 through out the impoundments. Oxidation zones developed both in the uphill and downhill impoundments to a depth of 5 m and are characterized by interlayering of coarse dark unoxidized layers with

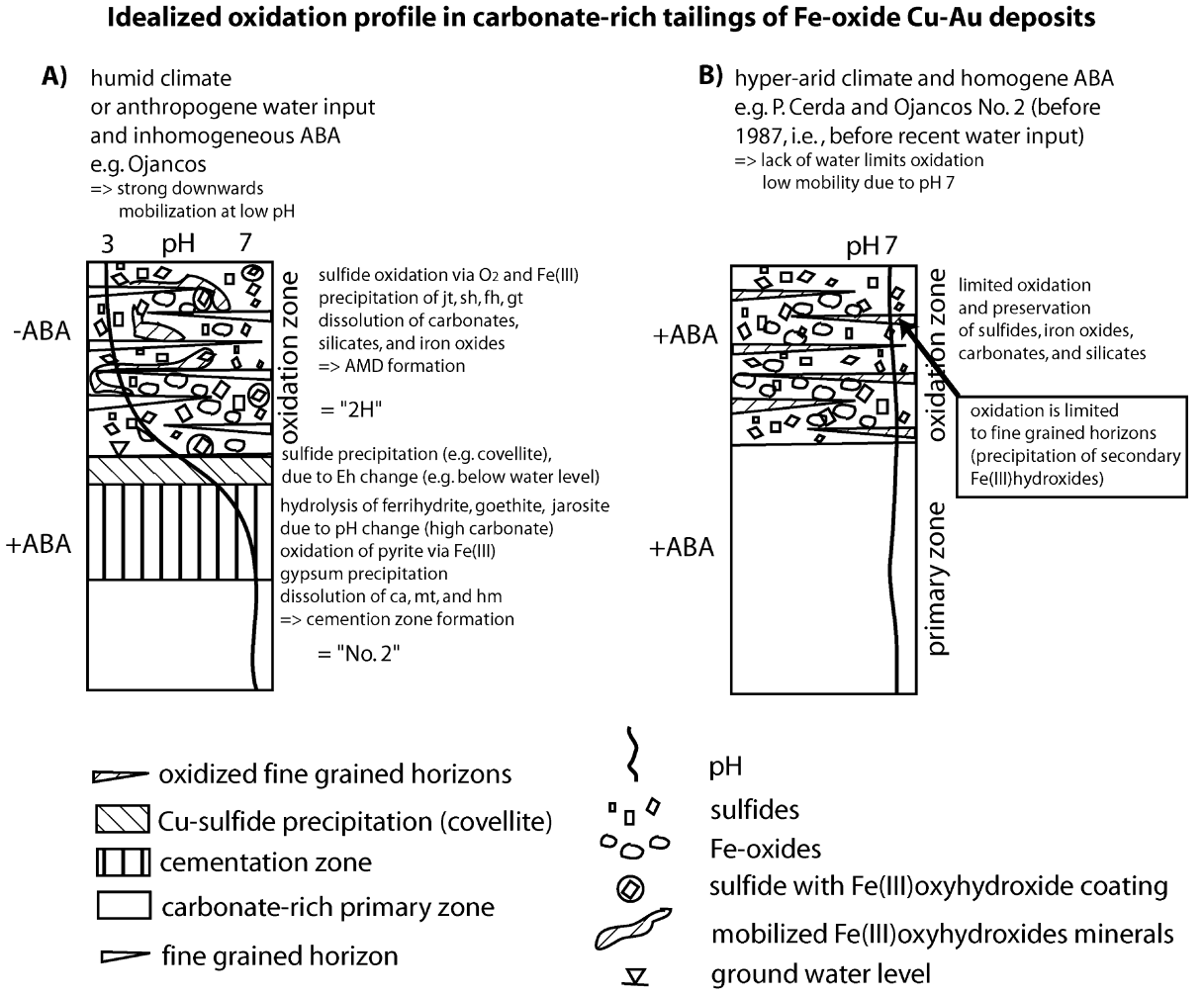

Fig. 14. (A) Schematic model of cemented zone formation at Ojancos, due to element leaching in a low-pH oxidation zone (− ABA at "2H") and precipitation of secondary phases when the acid solution reach carbonate-rich zone (+ABA at no. 2). The recent primary zone of Ojancos no. 2 is not represented. (B) Schematic model of a neutral pH oxidation zone (+ABA) development in hyperarid climate as observed at P. Cerda and in the Ojancos no. 2 tailings.

fine-grained, Fe(III)hydroxide-rich, ochre to red-brown colored oxidized horizons and by extensive preservation of sulfide and oxide minerals. As the tailings are located in a hyperarid climate, the coarse horizons dry out first and the oxidation takes place predominantly in the fine-grained horizons, relatively richer in moisture. This indicates that the hyperarid climate of the Atacama desert is limiting the availability of the acid potential, as most of the sulfides are in the coarser horizons due to gravity separation. However, results indicate that during operation an important element transfer from the younger upstream tailings to the older downstream tailings impoundment took place, possibly by sorptive transport at ferric polymers or colloids in form of neutral mine drainage (NMD). An additional source of ferric iron may be the dissolution of magnetite and hematite by CO_3 complexation at neutral to alkaline pH conditions (Bruno and Duro, 2000; Bruno et al., 1992; Hummel, 2000), i.e., a process different to the one described above for Ojancos, where most likely acid dissolution of magnetite and hematite play the predominant role.

Due to high water input during operation of the uphill impoundment no. 6, a constant water flow downstream is assumed, in a similar way as observed during sampling at Ojancos. The neutral pH will have the effect that the liberated metal cations and anions will adsorb to the ferric polymers and may be transported downstream to the older impoundment no. 4, leading to the formation of cementation zone. This would explain the metals enrichments in the cementation zone, which are mainly associated to the exchangeable fraction and not as secondary sulfides. After operation, no water-soluble sulfate minerals were formed at the tailings surface, as neutral pH and low water content limit the mobility of the liberated metals.

This study illustrates how metal transport can be made even with neutral oxidation zones. It also shows that the behavior of oxidation zones is dependent on climate and grain size. For examsple, in humid climates, the coarse horizons of the low-pH oxidation zones of porphyry coppers show stronger sulfide oxidation and mobilization than the fine horizons. This is due to the fact that the coarse horizons have a higher sulfide content and allow higher water and oxygen transport (Dold and Fontboté, 2001). In contrast, the study of the neutral oxidation zones at P. Cerda and of the neutral oxidation zone at the downhill Ojancos no. 2 impoundment indicate that the lack of water in the hyperarid climate of the Atacama desert decreases the sulfide oxidation rate and that oxidation takes place preferentially at the fine-grained, sulfide poor horizons, because of their higher water retention capacity. The mobility is additionally limited in the case of high pH conditions as in the oxidation zones at P. Cerda and no upwards transport and deposition of efflorescent salts can develop.

The impoundment construction and the associated anthropogenic water input may also strongly influence element transfer. Both at the downhill impoundments at Ojancos and P. Cerda, most element mobilization is not related to seepage from the oxidation zones characterized by neutral pH but to seepage from more recent tailings located uphill. The comparative study of these two case studies also shows the importance of the homogeneous versus inhomogeneous distribution of the neutralization potential to prevent the formation of AMD and to explain the formation of cementation zones. The downhill impoundment at Ojancos, characterized by alternating neutralizing and acid producing zones illustrates how carbonate-rich zones can control the retention of the mobilized elements and the formation of cemented zones. When operation will cease, the distribution of the carbonates will also control the element mobility.

The present study also illustrates that a detailed study of the processes taking place in tailings from carbonate-rich Fe-oxide Cu–Au deposits is necessary before making assessments on potential of acid drainage and element mobility. Factors like carbonate, sulfide and iron oxide distribution (and not only content), impoundment construction techniques and related anthropogenic water input into older tailings, grain size and climate must be taken in account. Thus, a detailed study will required to evaluate the necessity of incorporating basal liners or other constructive devices or adding lime and how this should be done. For example, in certain cases a carbonate layer at the bottom of the impoundment may induce the formation of a self-sealing cementation zone to prevent or reduce the long-term seepage of AMD and at the same time can control the enrichment of mobilized elements (e.g., Cu) for possible later recovery. Additionally, the case of P. Cerda has shown how effective a carbonate-rich layer at the top of the tailings can limit the mobility of the elements and so prevent the formation of water-soluble salts at the top of the tailings in arid climates.

8. Conclusion

In tailings from the Punta del Cobre District, as from other carbonate rich Fe oxide Cu–Au deposits, the primary mineralogy is characterized by variable content of pyrite and chalcopyrite with relatively high magnetite and/or hematite content. Gangue is dominantly calcite with minor quartz. The host silicate assemblage, largely controlled by hydrothermal alteration consists of K-feldspar ± Ca-amphibole ± biotite ± sericite ± chlorite ± tourmaline ± epidote ± quartz. This mineral assemblage offers two sources of Fe(III): on one side pyrite (2–4 wt.%) and chalcopyrite oxidation, on the other side iron oxide dissolution (hematite and magnetite) via either acid dissolution or, in carbonate controlled systems (pH 7), via CO_3 complexation. Fe(III) is a very effective oxidant for the

sulfide oxidation itself and a potential source of acidity in case of hydrolysis to Fe(III)oxyhydroxides. The host-rock assemblage has low neutralization potential and slow reactivity. Thus, the very variable carbonate (3–40 wt.% calcite) content provides the main neutralization potential in this deposit type, which is characterized by a high variability of the ABA. At both studied sites (Ojancos and P. Cerda), tailings filled valley dam impoundments. After ceasing operation of the older impoundments, new tailings were deposited upstream. This resulted in seepage migration from the upstream new tailings into the older downstream tailings impoundment.

In the case of Ojancos, the upstream new tailings "2H" have an − ABA, resulting in the seepage of AMD into the downstream no. 2 tailings (schwertmannite and chalcoalumite precipitation at the AMD out flow). Thus, sulfides (pyrite, chalcopyrite), iron oxides (magnetite, hematite) and carbonates (calcite) are destroyed in "2H" during oxidation and dissolution processes and the elements are transferred to the older tailings. High carbonate containing horizons (+ ABA) initiate the formation of a low-permeable cementation zone where they are enriched as secondary precipitates (e.g., ferrihydrite, goethite, jarosite, gypsum and covellite) or by pH controlled sorption processes.

If the carbonates are homogeneously distributed and the ABA is positive (case of P. Cerda), the produced acidity via sulfide oxidation is neutralized (pH 7) and so the mobility of most of the liberated elements is limited (exception are elements stable as oxyanions, e.g., As, SO_4). However, results indicate that during operation an important element transfer from the younger upstream tailings to the older downstream tailings impoundment took place, possibly by sorptive transport at ferric polymers or colloids in form of neutral mine drainage (NMD), resulting in a similar cementation zone as at Ojancos.

The water has two functions in sulfide oxidation: reactant and transport media. In the hyperarid Atacama desert, where the studied tailings are located, the natural precipitation input is negligible (20 mm/year). Thus, oxidation takes place predominantly in the fine-grained, relatively richer in moisture horizons, whereas oxidation of the coarse, sulfide-rich horizons of the tailings is limited, diminishing the acid potential. However, the observed practice of constructing new valley dam impoundments uphill of older ones, and allowing seepage of water and AMD from the recent into the older tailings, increases significantly the acid potential and the element mobility of the older tailings.

Acknowledgements

We thank E.H. Oelkers, Bo Strömberg and an anonymous reviewer for the helpful remarks on the manuscript. We especially thank the management and all staff involved in this project from Cía. Minera Sali Hochschild and Cía. Minera Ojos del Salado for their interest, access to the properties, logistic support and collaboration, especially B. Zamora (Planta Ojancos, Compañia Minera Sali Hochschild), W. Rojas (Compañia Minera Ojos del Salado) and C. Strickler (Phelps Dodge). Support in Chile during field work, sampling, sample preparation and analytical procedures by G. Cáceres, K. Eppinger and their staff (IDICTEC-University of Atacama), R. Troncoso, A. Hauser, C. Reuschmann, C. Espejo, E. Fonseca, W. Vivallio, I. Aguirre (Servicio Nacional de Geología y Minería, SERNAGEOMIN), W. Eberle and H.W. Müller (Bundesanstalt für Geowissenschaften und Rohstoffe BGR) is acknowledged. The project was supported by the German Academic Exchange Service (DAAD) and the Swiss National Science Foundation project no. 21-50778.97. **[EO]**

References

Andersson, P.S., Porcelli, D., Gustafsson, O., Ingri, J., Wasserburg, G.J., 2001. The importance of colloids for the behavior of uranium isotopes in the low-salinity zone of a stable estuary. Geochimica et Cosmochimica Acta 65 (1), 13–25.

Bigham, J.M., Schwertmann, U., Carlson, L., Murad, E., 1990. A poorly crystallized oxyhydroxysulfate of iron formed by bacterial oxidation of Fe(II) in acid mine waters. Geochimica et Cosmochimica Acta 54, 2743–2758.

Bigham, J.M., Carlson, L., Murad, E., 1994. Schwertmannite, a new iron oxyhydroxy-sulphate from Pyhäsalmi, Finland, and other localities. Mineralogical Magazine 58, 641–648.

Bigham, J.M., Schwertmann, U., Traina, S.J., Winland, R.L., Wolf, M., 1996. Schwertmannite and the chemical modeling of iron in acid sulfate waters. Geochimica et Cosmochimica Acta 60 (12), 2111–2121.

Blowes, D.W., Jambor, J.L., Hanton-Fong, C.J., Lortie, L., Gould, W.D., 1998. Geochemical, mineralogical and microbiological

characterization of a sulphide-bearing carbonate-rich gold-mine tailings impoundment, Joutel, Quebec. Applied Geochemistry 13 (6), 687–705.

Brookins, D.G., 1988. Eh–pH Diagrams for Geochemistry. Springer, Berlin, 176 pp.

Bruno, J., Duro, L., 2000. Reply to W. Hummel's comment on and correction to "On the influence of carbonate in mineral dissolution: 1. The thermodynamics and kinetics of hematite dissolution in bicarbonate solutions at $T=25$ °C" by J. Bruno, W. Stumm, P. Wersin, and F. Brandberg. Geochimica et Cosmochimica Acta 64 (12), 2173–2176.

Bruno, J., Wersin, P., Stumm, W., 1992. On the influence of carbonate in mineral dissolution: II. The solubility of $FeCO_3$(s) at 25 °C and 1 atm total pressure. Geochimica et Cosmochimica Acta 56, 1149–1155.

Chao, T.T., Sanzolone, R.F., 1977. Chemical dissolution of sulfide minerals. Journal of Research of the U.S. Geological Survey 5, 409–412.

Chen, J.Y., Ko, C.H., Bhattacharjee, S., Elimelech, M., 2001. Role of spatial distribution of porous medium surface charge heterogeneity in colloid transport. Colloids and Surfaces, A: Physicochemical and Engineering Aspects 191 (1–2 Special Issue SI), 3–15.

Cornell, R.M., Schwertmann, U., 1996. The Iron Oxides. VCH Verlagsgesellschaft, Weinheim, 573 pp.

Dold, B., 1999. Mineralogical and geochemical changes of copper flotation tailings in relation to their original composition and climatic settings—implications for acid mine drainage and element mobility. PhD thesis, Terre & Environment, University of Geneva, Geneva, 230 pp.

Dold, B., 2001a. A 7-step sequential extraction for geochemical studies of copper sulfide mine waste, securing the future. International Conference on Mining and the Environment, Skellefteå, Sweden, 158–170.

Dold, B., 2001b. Dissolution kinetics of schwertmannite and ferrihydrite, securing the future. International Conference on Mining and the Environment, Skellefteå, Sweden, pp. 171–181.

Dold, B., Fontboté, L., 2001. Element cycling and secondary mineralogy in porphyry copper tailings as a function of climate, primary mineralogy, and mineral processing. Special issue: geochemical studies of mining and the environment. Journal of Geochemical Exploration 74 (1–3), 3–55.

Dold, B., Eppinger, K.J., Kölling, M., 1996. Pyrite oxidation and the associated geochemical processes in tailings in the atacama desert/Chile: the influence of men controlled water input after disuse. In: Sanchez, M.A., Vergara, F., Castro, S.H. (Eds.), Clean Technology for the Mining Industry, Santiago. University of Concepción, Chile, pp. 417–427.

Dzombak, D.A., Morel, F.M.M., 1990. Surface Complexation Modeling—Hydrous Ferric Oxides. Wiley, New York, 393 pp.

Evangelou, V.P., Huang, X., 1994. Infrared spectroscopy evidence of an iron(II)–carbonate complex on the surface of pyrite. Spectrochimica Acta 50 (A), 1333.

Fanfani, L., Zuddas, P., Chessa, A., 1997. Heavy metals speciation analysis as a tool for studying mine tailings weathering. Journal of Geochemical Exploration 58, 241–248.

Fonseca, E., Martin, H., 1986. The selective extraction of Pb and Zn in selected mineral and soil samples, application in geochemical exploration (Portugal). Journal of Geochemical Exploration 26, 231–248.

Gatehouse, S., Roussel, D.W., Van Moort, J.C., 1977. Sequential soil analysis in exploration analysis. Journal of Geochemical Exploration 8, 483–494.

Hall, G.E.M., Vaive, J.E., Beer, R., Hoashi, M., 1996. Selective leaches revisited, with emphasis on the amorphous Fe oxyhydroxide phase extraction. Journal of Geochemical Exploration 56, 59–78.

Holmström, H., Ljungberg, J., Öhlander, B., 1999. Role of carbonates in mititgation of metal release from mining waste. Evidence from humidity cells tests. Environmental Geology 37 (4), 267–280.

Hölting, B., 1989. Hydrogeologie. Enke, Stuttgart, 396 pp.

Hummel, W., 2000. Comment on "On the influence of carbonate in mineral dissolution: 1. The thermodynamics and kinetics of hematite dissolution in bicarbonate solutions at $T=25$ °C" by J. Bruno, W. Stumm, P. Wersin, and F. Brandberg. Geochimica et Cosmochimica Acta 64 (12), 2167–2171.

Jambor, J.L., 1994. Mineralogy of sulfide-rich tailings and their oxidation products. In: Jambor, J.L., Blowes, D.W. (Eds.), Short Course Handbook on Environmental Geochemistry of Sulfide Mine-Waste. Mineralogical Association of Canada, Nepean, pp. 59–102.

Lapakko, K., Antonson, D.A., Wagner, J.R., 1997. Mixing of limestone with finely-crushed acid producing rock. ICARD, Vancouver, 1345–1360.

Marschik, R., 1996. Cretaceous Cu(–Fe) mineralization in the Punta del Cobre belt, Nothern Chile. PhD thesis, Terre & Environment, University of Geneva, Geneva, 200 pp.

Marschik, R., Fontboté, L., 1996. Copper(–iron) mineralization and superposition of alteration events in the Punta del Cobre belt, northern Chile. Economic Geology, Special Publication 5, 171–189.

Marschik, R., Fontboté, L., 2001a. The Candelaria–Punta del Cobre iron oxide Cu–Au(–Zn–Ag) deposits. Economic Geology 96 (8), 1799–1826.

Marschik, R., Fontboté, L., 2001b. The Punta del Cobre Formation, Punta del Cobre–Candelaria area, northern Chile. Journal of South American Earth Sciences 14 (4), 401–433.

Moore, D.M., Reynolds, R.C., 1997. X-ray Diffraction and the Identification and Analysis of Clay Minerals. Oxford Univ. Press, Oxford. 378 pp.

Moses, C.O., Nordstrom, D.K., Herman, J.S., Mills, A.L., 1987. Aqueous pyrite oxidation by dissolved oxygen and by ferric iron. Geochimica et Cosmochimica Acta 51, 1561–1571.

Nordstrom, D.K., Alpers, C.N., 1999. Geochemistry of acid mine waste. In: Plumlee, G.S., Logsdon, M.J. (Eds.), The Environmental Geochemistry of Ore Deposits. Part A: Processes, Techniques, and Health Issues. Reviews in Economic Geology. Society of Economic Geologists, Littleton, pp. 133–160.

Ren, J.H., Packman, A.I., Welty, C., 2001. Analysis of an observed relationship between colloid collision efficiency and mean collector grain size. Colloids and Surfaces, A: Physicochemical and Engineering Aspects 191 (1–2 Special Issue SI), 133–144.

Ribet, I., Ptacek, C.J., Blowes, D.W., Jambor, J.L., 1995. The po-

tential for metal release by reductive dissolution of weathered mine tailings. Journal of Contaminant Hydrology 17 (3), 239–273.

Ryan, P.J., et al., 1995. The Candelaria copper–gold deposit, Chile. In: Pierce, F.W., Bolm, J.G. (Eds.), Porphyry Copper Deposits of the American Cordillera. Arizona Geological Society Digest. Arizona Geological Society, Tucson, pp. 625–645.

Samson, S.D., Eggleston, C.M., 2000. The depletion and regeneration of dissolution-active sites at the mineral–water interface: II. Regeneration of active sites on [alpha]-Fe_2O_3 at pH 3 and pH 6. Geochimica et Cosmochimica Acta 64 (21), 3675–3683.

Schulze, D.G., 1981. Identification of soil iron oxides minerals by differential X-ray diffraction. Soil Science Society of America Journal 45, 437–440.

Schulze, D.G., 1994. Differential X-ray diffraction analysis of soil material. Quantitative Methods in Soil Mineralogy. SSSA Miscellaneous Publication. Soil Science Society of America, pp. 412–429.

Schwertmann, U., 1964. Differenzierung der Eisenoxide des Bodens durch Extraktion mit Ammoniumoxalat Lösung. Zeitschrift für Pflanzenernährung und Bodenkunde 105, 194–202.

Schwertmann, U., Bigham, J.M., Murad, E., 1995. The first occurence of schwertmannite in a natural stream environment. European Journal of Mineralogy 7, 547–552.

Schwertmann, U., Friedl, J., Stanjek, H., 1999. From Fe(III) ions to ferrihydrite and then to hematite. Journal of Colloid and Interface Science 209, 215–223.

Sondag, F., 1981. Selective extraction procedures applied to geochemical prospecting in an area contaminated by old mine workings. Journal of Geochemical Exploration 15, 645–652.

Stone, A.T., 1987. Microbial metabolites and the reductive dissolution of manganese oxides: oxalate and pyruvate. Geochimica et Cosmochimica Acta 51, 919–925.

Tessier, A., Campbell, P.G.C., Bisson, M., 1979. Sequential extraction procedure for speciation of particulate trace metals. Analytical Chemistry 51, 844–851.

Webster, J.G., Swedlund, P.J., Webster, K.S., 1998. Trace metal adsorption onto an acid mine drainage iron(III)oxyhydry sulfate. Environmental Science and Technology 32 (10), 1362–1368.

White III, W.W., Lapakko, K.A., Cox, R.L. 1999. Static-test methods most commonly used to predict acid mine drainage: practical guidelines for use and interpretation. In: Plumlee, G.S., Logsdon, M.J. (Eds.), The Environmental Geochemistry of Ore Deposits. Part A: Processes, Techniques, and Health Issues-Reviews in Economic Geology. Society of Economic Geologists, Littleton, pp. 325–338.

Zamora, B., 1993. Antecedentes para monografia de Compañia Minera y Comercial Sali Hochschild, Copiapó.